

Mixed soliton solutions of the defocusing nonlocal nonlinear Schrödinger equation

Tao Xu^{1,2,*}, Sha Lan², Min Li^{3,†}, Ling-Ling Li², Guo-Wei Zhang²

1. State Key Laboratory of Heavy Oil Processing,

China University of Petroleum, Beijing 102249, China

2. College of Science, China University of Petroleum, Beijing 102249, China

3. School of Mathematics and Physics,

North China Electric Power University, Beijing 102206, China

Abstract

By using the Darboux transformation, we obtain two new types of exponential-and-rational mixed soliton solutions for the defocusing nonlocal nonlinear Schrödinger equation. We reveal that the first type of solution can display a large variety of interactions among two exponential solitons and two rational solitons, in which the standard elastic interaction properties are preserved and each soliton could be either the dark or antidark type. By developing the asymptotic analysis method, we also find that the second type of solution can exhibit the elastic interactions among four mixed asymptotic solitons. But in sharp contrast to the common solitons, the mixed asymptotic solitons have the t -dependent velocities and their phase shifts before and after interaction also grow with $|t|$ in the logarithmical manner. In addition, we discuss the degenerate cases for such two types of mixed soliton solutions when the four-soliton interaction reduces to a three-soliton or two-soliton interaction.

Keywords: Nonlocal nonlinear Schrödinger equation; Mixed soliton solutions; Soliton interactions; Darboux transformation; Asymptotic analysis

PACS numbers: 05.45.Yv; 02.30.Ik

*Corresponding author, e-mail: xutao@cup.edu.cn

†Corresponding author, e-mail: micheller85@126.com

1 Introduction

Recently, it has become an active topic to study the integrable nonlocal evolution equations in nonlinear mathematical physics and soliton theory. In 2013, Ablowitz and Musslimani first proposed the following nonlocal nonlinear Schrödinger (NLS) equation [1]:

$$iu_t = u_{xx} + 2\varepsilon u^2 \bar{u} \quad (\varepsilon = \pm 1), \quad (1)$$

where u is a complex-valued function of real variables x and t , $\varepsilon = 1$ and $\varepsilon = -1$ represent, respectively, the focusing (+) and defocusing (−) nonlinearity, and the *bar* denotes the combination of complex conjugate and space reversal, i.e., $\bar{u} = u^*(-x, t)$. Compared with the standard (local) NLS equation, the cubic nonlinear term $|u|^2 u$ is replaced with $u^2 \bar{u}$, so that the evolution dynamics of the field in Eq. (1) is non-locally dependent on the values of u at both the positions x and $-x$. Also, this equation is said to be parity-time (\mathcal{PT}) symmetric since it is invariant under the combined action of parity operator \mathcal{P} ($x \rightarrow -x$) and time-reversal operator \mathcal{T} ($t \rightarrow -t, i \rightarrow -i$). As a matter of fact, Eq. (1) can be viewed as a linear \mathcal{PT} -symmetric Schrödinger equation $iu_t = u_{xx} + V(x, t)u$ with the self-induced potential $V(x, t) = 2\varepsilon u\bar{u}$ satisfying the \mathcal{PT} -symmetric relation $V(x, t) = V^*(-x, t)$. This makes Eq. (1) relate to the \mathcal{PT} -symmetric physics [2], and may bring potential applications in some unconventional physical systems [3, 4].

It is remarkable that Eq. (1) is a Hamiltonian integrable model in the sense of admitting the Lax pair and an infinite number of conservation laws, and that its initial-value problem can be solved via the inverse scattering transform (IST) [1, 5–9]. In the past few years, this equation has attracted intensive attention and its integrable properties and solution dynamics have been studied from different points of view. Some progresses have been made in the following aspects: the IST scheme for solving Eq. (1) with nonzero boundary conditions [7], gauge equivalence to the unconventional system of coupled Landau-Lifshitz equations [4], complete integrability of a whole hierarchy of nonlocal NLS equations [10], long-time asymptotic behavior of the solution with decaying boundary conditions [11], connection between nonlocal and local NLS equations through the variable transformation [12], exact soliton and rogue-wave solutions by different analytical methods [1, 3, 5–7, 13–26]. In addition, by considering the parity/time reversal, charge conjugation, space/time translation and their proper combinations, many other integrable nonlocal models have been obtained from their local counterparts. Typical examples include the nonlocal reverse space-time NLS equation [8], semi-discrete NLS equation [27], vector (or multi-component) NLS equation [28, 29], derivative NLS equation [30, 31], modified Korteweg-de Vries equation [5, 6, 32], sine-Gordon equation [5, 6, 9], Davey-Stewartson (DS) equation [6, 33], N -wave system [34], Sasa-Satsuma equation [35] and various nonlocal Alice-Bob systems [36, 37].

As shown in the previous studies [1, 3, 5–7, 13–25], the nonlocal NLS equation possesses abundant localized-wave solutions and their dynamical behaviors are distinguished from those in the local counterpart. The focusing nonlocal NLS equation has the bright-soliton, dark-soliton, rogue-wave and breather solutions [1, 3, 13, 21–23], simultaneously. Those solutions are bounded only for some particular parametric choices, but they in general develop the collapsing singularities in finite time [1, 5, 22, 23]. For the defocusing case, Eq. (1) admits the exponential soliton solutions as well as the rational soliton solutions on the same continuous wave (cw) background $u_{\text{cw}} = \rho e^{i(2\rho^2 t + \phi)}$ (with $\rho \neq 0$ and ϕ being two real parameters) [7, 14–18]. Both types of soliton solutions can display a rich variety of elastic interactions and each asymptotic soliton could be either the dark or antidark type. In contrast to the standard elastic soliton interactions, some unusual interaction properties have been revealed: the exponential N -soliton solution contains generally $2N$ interacting solitons [14]; the rational soliton experiences no phase shift when interacting with another rational one [15]; the asymptotic solitons in the higher-order rational solutions have the t -dependent velocities because their center trajectories are localized in some curves in the xt plane [16]. However, whether for the focusing or defocusing nonlocal NLS equation, the stability of localized-wave solutions can be easily destroyed if there is a small shift for the initial value in the x coordinate [3, 14, 15].

It is known that the Darboux transformation (DT) is an algebraic iterative method which can generate an infinite chain of explicit solutions for the Lax integrable equations from a trivial seed [38]. Lately, we have succeeded in constructing the exponential and rational soliton solutions of the defocusing nonlocal NLS equation [14, 15] by the elementary and generalized DTs. If the potential is given by the cw solution $\rho e^{i(2\rho^2 t + \phi)}$, the Lax pair of Eq. (1) with $\varepsilon = -1$ usually has the solution in the exponential form (see Eq. (14) below), but such solution will reduce to a rational one (see Eq. (15) below) when the spectral parameter takes the critical value $\lambda = i\sigma\rho$ ($\sigma = \pm 1$). As a result, the elementary DT can be used to derive the exponential soliton solutions based on a set of N linearly independent solutions at different spectral parameters $\{\lambda_k\}_{k=1}^N$ with $\lambda_k \neq i\sigma\rho$ [14], while the generalized DT can generate the rational soliton solutions when all λ_k 's degenerate to $i\sigma\rho$ [15]. However, it is also possible for N spectral parameters to partially degenerate to $i\sigma\rho$ or the degeneration occurs at any non-critical value. That is to say, quite a number of degenerate cases have been overlooked in the existing literature although they can still be dealt with via the generalized DT. With this consideration at $N = 2$, we in this paper construct two new types of exponential-and-rational mixed soliton solutions for the defocusing nonlocal NLS equation. We reveal that the first type of solution can display a large variety of elastic interactions, in which there are in general two exponential solitons and two rational solitons, and each interacting soliton could be either the dark or antidark type. For the second type of solution, we develop the asymptotic analysis method and find that the solutions contain four mixed asymptotic solitons and each one can also display the dark or antidark soliton

profile. Very specially, all the center trajectories of mixed solitons are localized in some curves in the xt plane, so that they have the t -dependent velocities and their phase shifts before and after interaction grow with $|t|$ in a logarithmical manner.

The structure of this paper is organized as follows: In Section 2, we review the elementary and generalized DTs of Eq. (1), as proposed in Refs. [14, 15]. In Section 3, for the case $\lambda_1 = ib\rho$ ($0 < |b| < 1$) and $\lambda_2 = i\sigma\rho$, we use the elementary DT to construct the first type of mixed soliton solution, and reveal the elastic soliton interaction properties through an asymptotic analysis. In Section 4, for another case $\lambda_2, \lambda_1 \rightarrow ib\rho$ ($0 < |b| < 1$), we derive the second type of mixed soliton solution by the generalized DT. Specially, we develop the asymptotic analysis method and obtain some uncommon soliton interaction properties which have never been reported before. In Section 5, we address the conclusions and discussions of our work.

2 Darboux Transformation

As a special gauge transformation leaving the form of Lax pair invariant, the DT comprises of the eigenfunction and potential transformations [38, 39]. Since Eq. (1) is an integrable model, it has the Lax pair in the form [1]:

$$\Psi_x = U\Psi = \begin{pmatrix} \lambda & u(x, t) \\ -\varepsilon u^*(-x, t) & -\lambda \end{pmatrix} \Psi, \quad (2a)$$

$$\Psi_t = V\Psi = \begin{pmatrix} -2i\lambda^2 - i\varepsilon u(x, t)u^*(-x, t) & -2i\lambda u(x, t) - iu_x(x, t) \\ 2i\varepsilon\lambda u^*(-x, t) - i\varepsilon u_x^*(-x, t) & 2i\lambda^2 + i\varepsilon u(x, t)u^*(-x, t) \end{pmatrix} \Psi, \quad (2b)$$

where $\Psi = (f, g)^T$ (the superscript T represents the vector transpose) is the vector eigenfunction, λ is the spectral parameter, and Eq. (1) can be recovered from the compatibility condition $U_t - V_x + UV - VU = 0$.

Assume that $\Psi_k = [f_k(x, t), g_k(x, t)]^T$ ($1 \leq k \leq N$) are N linearly-independent solutions of Eqs. (2a) and (2b) with different spectral parameters λ_k ($1 \leq k \leq N$), where λ_k cannot be taken as a real number to avoid the trivial iteration of the DT. One can check that $\bar{\Psi}_k = [g_k^*(-x, t), \varepsilon f_k^*(-x, t)]^T$ also solves Eqs. (2a) and (2b) with $\lambda = \lambda_k^*$. Based on the work in Ref. [14], the N th-iterated elementary DT can be constituted by the eigenfunction transformation

$$\Psi_{[N]} = T_{[N]}\Psi, \quad T_{[N]} = \begin{pmatrix} \lambda^N - \sum_{n=1}^N a_n(x, t)\lambda^{n-1} & -\sum_{n=1}^N b_n(x, t)(-\lambda)^{n-1} \\ -\sum_{n=1}^N c_n(x, t)\lambda^{n-1} & \lambda^N - \sum_{n=1}^N d_n(x, t)(-\lambda)^{n-1} \end{pmatrix} \quad (3)$$

and the potential transformation

$$u_{[N]}(x, t) = u(x, t) + 2(-1)^{N-1}b_N, \quad u_{[N]}^*(-x, t) = u^*(-x, t) + 2\varepsilon c_N. \quad (4)$$

The functions $a_n(x, t)$, $b_n(x, t)$, $c_n(x, t)$ and $d_n(x, t)$ ($1 \leq n \leq N$) are uniquely determined by

$$T_{[N]} |_{\lambda=\lambda_k} \Psi_k = \mathbf{0}, \quad T_{[N]} |_{\lambda=\lambda_k^*} \bar{\Psi}_k = \mathbf{0} \quad (1 \leq k \leq N), \quad (5)$$

and particularly b_N and c_N can be represented as

$$b_N = (-1)^{N-1} \frac{\tau_{N+1, N-1}}{\tau_{N, N}}, \quad c_N = \frac{\tau_{N-1, N+1}}{\tau_{N, N}}, \quad (6)$$

with

$$\tau_{M, L} = \begin{vmatrix} F_{N \times M} & G_{N \times L} \\ \varepsilon \bar{G}_{N \times M} & \bar{F}_{N \times L} \end{vmatrix} \quad (M + L = 2N), \quad (7)$$

where the block matrices $F_{N \times M} = [\lambda_k^{m-1} f_k(x, t)]_{\substack{1 \leq k \leq N, \\ 1 \leq m \leq M}}$, $G_{N \times L} = [(-\lambda_k)^{m-1} g_k(x, t)]_{\substack{1 \leq k \leq N, \\ 1 \leq m \leq L}}$, $\bar{G}_{N \times M} = [\lambda_k^{*m-1} g_k^*(-x, t)]_{\substack{1 \leq k \leq N, \\ 1 \leq m \leq M}}$ and $\bar{F}_{N \times L} = [(-\lambda_k^*)^{m-1} f_k^*(-x, t)]_{\substack{1 \leq k \leq N, \\ 1 \leq m \leq L}}$.

We notice that the elementary DT cannot apply to the degenerate cases when some of the spectral parameters $\{\lambda_k\}_{k=1}^N$ coincide with each other because the coefficient matrix in Eq. (5) becomes singular. This difficulty may be overcome by the idea of Matveev's generalized DT [40, 41]. Let us consider the following general case:

$$\lambda_{k_1+1}, \dots, \lambda_{k_2-1} \rightarrow \lambda_{k_1}, \quad \lambda_{k_2+1}, \dots, \lambda_{k_3-1} \rightarrow \lambda_{k_2}, \dots, \lambda_{k_n+1}, \dots, \lambda_N \rightarrow \lambda_{k_n}, \quad (8)$$

where $1 = k_1 < k_2 < \dots < k_n \leq N$ ($\lambda_{k_i} \neq \lambda_{k_j}$, $1 \leq i < j \leq n$, $1 \leq n \leq N$). For convenience, we define that $l_i = k_{i+1} - k_i - 1$ for $1 \leq i \leq n-1$ and $l_n = N - k_n$, and assume that

$$f_{k_i+h}(x, t) = f_{k_i}(x, t, \lambda_{k_i+h}), \quad g_{k_i+h}(x, t) = g_{k_i}(x, t, \lambda_{k_i+h}), \quad (9)$$

where $\lambda_{k_i+h} = \lambda_{k_i} + \epsilon_i$, $1 \leq h \leq l_i$ ($l_i > 0$), ϵ_i 's are small parameters. By expanding $\lambda_{k_i+h}^{m-1} f_{k_i}$ and $\lambda_{k_i+h}^{m-1} g_{k_i}$ in the Taylor series of ϵ_i and taking the limit $\epsilon_i \rightarrow 0$, the functions $a_n(x, t)$, $b_n(x, t)$, $c_n(x, t)$ and $d_n(x, t)$ in $T_{[N]}$ can be uniquely solved from Eq. (5) again. As a result, the potential transformation is replaced by

$$u_{[N]}(x, t) = u(x, t) + 2 \frac{\tau'_{N+1, N-1}}{\tau'_{N, N}}, \quad u_{[N]}^*(-x, t) = u^*(-x, t) + 2 \varepsilon \frac{\tau'_{N-1, N+1}}{\tau'_{N, N}}, \quad (10)$$

with

$$\tau'_{M, L} = \begin{vmatrix} F'_{l_1 \times M} & G'_{l_1 \times L} \\ \vdots & \vdots \\ F'_{l_n \times M} & G'_{l_n \times L} \\ \varepsilon \bar{G}'_{l_1 \times M} & \bar{F}'_{l_1 \times L} \\ \vdots & \vdots \\ \varepsilon \bar{G}'_{l_n \times M} & \bar{F}'_{l_n \times L} \end{vmatrix} \quad (M + L = 2N), \quad (11)$$

in which the block matrices $F'_{l_i \times M} = \left[f_{k_i}^{(m-1,j)}(x,t) \right]_{\substack{0 \leq j \leq l_i, \\ 1 \leq m \leq M}}$, $G'_{l_i \times L} = \left[(-1)^{m-1} g_{k_i}^{(m-1,j)}(x,t) \right]_{\substack{0 \leq j \leq l_i, \\ 1 \leq m \leq L}}$, $\bar{G}'_{l_i \times M} = \left[g_{k_i}^{*(m-1,j)}(-x,t) \right]_{\substack{0 \leq j \leq l_i, \\ 1 \leq m \leq M}}$ and $\bar{F}'_{l_i \times L} = \left[(-1)^{m-1} f_{k_i}^{*(m-1,j)}(-x,t) \right]_{\substack{0 \leq j \leq l_i, \\ 1 \leq m \leq L}}$ ($1 \leq i \leq n$), and the functions $f_{k_i}^{(m-1,j)}$ and $g_{k_i}^{(m-1,j)}$ are defined by

$$f_{k_i}^{(m-1,j)}(x,t) = \frac{1}{j!} \frac{\partial^j [\lambda_{k_i+h}^{m-1} f_{k_i}(x,t, \lambda_{k_i+h})]}{\partial \lambda_{k_i+h}^j} \Big|_{\epsilon_i=0}, \quad (12)$$

$$g_{k_i}^{(m-1,j)}(x,t) = \frac{1}{j!} \frac{\partial^j [\lambda_{k_i+h}^{m-1} g_{k_i}(x,t, \lambda_{k_i+h})]}{\partial \lambda_{k_i+h}^j} \Big|_{\epsilon_i=0}, \quad (13)$$

where $1 \leq i \leq n$, $1 \leq m \leq N$, $1 \leq h \leq l_i$, and particularity $f_{k_i}^{(0,0)}(x,t) = f_{k_i}(x,t)$, $g_{k_i}^{(0,0)}(x,t) = g_{k_i}(x,t)$.

Therefore, we call Eqs. (3) and (10) the N th-iterated generalized DT, which is applicable to any choice of the spectral parameters $\{\lambda_k\}_{k=1}^N$ only if $\lambda_k \neq \lambda_k^*$. One should note that the potential transformation in Eq. (4) corresponds to the particular case of the generalized one in Eq. (10) when $n = N$.

With the cw solution $u_{\text{cw}} = \rho e^{i(2\rho^2 t + \phi)}$ (where $\rho \neq 0$ and ϕ are two real parameters) as a seed, we implement the DT-iterated algorithm for Eq. (1) with $\varepsilon = -1$. In this case, depending on the value of the spectral parameter, the Lax pair (2a) and (2b) has two different solutions:

$$\begin{pmatrix} f_k \\ g_k \end{pmatrix} = \begin{pmatrix} e^{\frac{2i\rho^2 t + i\phi}{2}} (\alpha_k e^{h_k \xi_k} + \beta_k e^{-h_k \xi_k}) \\ e^{-\frac{2i\rho^2 t + i\phi}{2}} \left[\frac{\alpha_k (h_k - \lambda_k)}{\rho} e^{h_k \xi_k} - \frac{\beta_k (h_k + \lambda_k)}{\rho} e^{-h_k \xi_k} \right] \end{pmatrix} \quad (\lambda_k \neq i\sigma\rho), \quad (14)$$

$$\begin{pmatrix} f_k \\ g_k \end{pmatrix} = \begin{pmatrix} e^{\frac{2i\rho^2 t + i\phi}{2}} [\alpha_k (x + 2\sigma\rho t) + \beta_k] \\ e^{-\frac{2i\rho^2 t + i\phi}{2}} [-i\alpha_k \sigma (x + 2\sigma\rho t) + \frac{\alpha_k}{\rho} - i\beta_k \sigma] \end{pmatrix} \quad (\lambda_k = i\sigma\rho), \quad (15)$$

where $\sigma = \pm 1$, $h_k = \sqrt{\lambda_k^2 + \rho^2}$, $\xi_k = x - 2i\lambda_k t$, and α_k and β_k are free complex parameters. If taking $\lambda_k = ib_k\rho$ with $0 < |b_k| < 1$ and $b_k \neq b_j$ for all $1 \leq k \leq N$, the potential transformation (4) can give rise to a chain of exponential soliton solutions [14]. Instead, if $\lambda_2, \dots, \lambda_N \rightarrow \lambda_1 = i\sigma\rho$ (which corresponds to $n = 1$ and $l_1 = N - 1$ in Eq. (8)), one can derive the rational soliton solutions from Eq. (10) [15]. It should be noted that Eq. (8) contains quite a number of other degenerate cases which have been overlooked in the previous studies. With $N = 2$ as an example, there are the following two cases remaining to be studied: (i) $\lambda_1 = ib\rho$ ($0 < |b| < 1$), $\lambda_2 = i\sigma\rho$; (ii) $\lambda_2, \lambda_1 \rightarrow ib\rho$ ($0 < |b| < 1$). In Sections 3 and 4, by considering such two degenerate cases, we will derive two new types of mixed soliton solutions and discuss the soliton interaction properties via asymptotic analysis.

3 The first type of mixed soliton solution

In this section, by letting $\lambda_1 = ib\rho$ ($0 < |b| < 1$) and $\lambda_2 = i\sigma\rho$ ($\sigma = \pm 1$), we use the elementary DT to obtain the exponential-rational mixed soliton solution as follows:

$$u = \rho e^{2i\rho^2 t + i\phi} + 2 \frac{\begin{vmatrix} f_1 & \lambda_1 f_1 & \lambda_1^2 f_1 & g_1 \\ f_2 & \lambda_2 f_2 & \lambda_2^2 f_2 & g_2 \\ -\bar{g}_1 & -\lambda_1^* \bar{g}_1 & -\lambda_1^{*2} \bar{g}_1 & \bar{f}_1 \\ -\bar{g}_2 & -\lambda_2^* \bar{g}_2 & -\lambda_2^{*2} \bar{g}_2 & \bar{f}_2 \end{vmatrix}}{\begin{vmatrix} f_1 & \lambda_1 f_1 & g_1 & -\lambda_1 g_1 \\ f_2 & \lambda_2 f_2 & g_2 & -\lambda_2 g_2 \\ -\bar{g}_1 & -\lambda_1^* \bar{g}_1 & \bar{f}_1 & -\lambda_1^* \bar{f}_1 \\ -\bar{g}_2 & -\lambda_2^* \bar{g}_2 & \bar{f}_2 & -\lambda_2^* \bar{f}_2 \end{vmatrix}}, \quad (16)$$

with

$$f_1 = \alpha_1 e^{i\rho^2 t + \frac{i\phi}{2}} (e^{\kappa\xi_1} + \gamma_1 e^{-\kappa\xi_1}), \quad (17a)$$

$$g_1 = \alpha_1 e^{-i\rho^2 t - \frac{i\phi}{2}} (e^{\kappa\xi_1 - i\theta} - \gamma_1 e^{-\kappa\xi_1 + i\theta}), \quad (17b)$$

$$f_2 = \alpha_2 e^{i\rho^2 t + \frac{i\phi}{2}} (\eta_1 + \gamma_2), \quad (17c)$$

$$g_2 = -\frac{i\alpha_2}{\rho} e^{-i\rho^2 t - \frac{i\phi}{2}} [\sigma\rho(\eta_1 + \gamma_2) + i], \quad (17d)$$

$$\xi_1 = x + 2b\rho t, \quad \eta_1 = x + 2\sigma\rho t, \quad \kappa = \rho\sqrt{1-b^2}, \quad (17e)$$

$$\theta = \arctan(b/\sqrt{1-b^2}), \quad \gamma_k = \beta_k/\alpha_k \quad (k = 1, 2), \quad (17f)$$

where $\bar{f}_k = f_k^*(-x, t)$, $\bar{g}_k = g_k^*(-x, t)$ ($k = 1, 2$), $-\pi/2 < \theta < \pi/2$, γ_1 and γ_2 are two complex parameters. Note that α_1 and α_2 will be canceled out when f_k and g_k ($k = 1, 2$) are substituted into Eq. (16). For convenience, we define $\gamma_1 = r_1 e^{i\varphi_1}$ with $-\pi < \varphi_1 \leq \pi$ and $r_1 > 0$ being a real constant.

3.1 Asymptotic analysis

We use the asymptotic analysis method to study the soliton interactions described by solution (16). It turns out that solution (16) has four different asymptotic soliton states when $|t| \rightarrow \infty$, which are given as follows:

- (i) If $\xi_1 = x + 2b\rho t = O(1)$, from $\bar{\xi}_1 = -\xi_1 + 4b\rho t$ we have $\bar{\xi}_1 \rightarrow \pm\infty$ as $\text{sgn}(b)t \rightarrow \pm\infty$. Then, calculating the limit of solution (16) when $\bar{\xi}_1 \rightarrow \pm\infty$ gives the following asymptotic expression in

the exponential form

$$u \rightarrow \begin{cases} u_1^+ = \rho e^{2i\rho^2 t + i\phi} \left[1 + \frac{i(1 + e^{2i\theta})}{b r_1 e^{-2\kappa\xi_1 + i(\theta + \varphi_1)} - i} \right] & (\text{sgn}(b)t \rightarrow \infty), \\ u_1^- = \rho e^{2i\rho^2 t + i\phi} \left[1 - \frac{i(1 + e^{-2i\theta})}{b r_1^{-1} e^{2\kappa\xi_1 - i(\theta + \varphi_1)} + i} \right] & (\text{sgn}(b)t \rightarrow -\infty), \end{cases} \quad (18a)$$

$$|u| \rightarrow |u_1^\pm| = \rho \left[1 + \frac{2\sqrt{1 - b^2} \sin(\varphi_1)}{\text{sgn}(b) \cosh(2\kappa\xi_1 + \Delta_1^\pm) - \sin(\theta + \varphi_1)} \right]^{\frac{1}{2}}, \quad (18b)$$

with $\Delta_1^\pm = -\ln(r_1 |b|^{\pm 1})$. It can be seen from Eq. (18b) that u_1^\pm has no singularity if and only if γ_1 and b satisfy

$$\sin(\theta + \varphi_1) \neq \text{sgn}(b), \quad (19)$$

and it is localized in the line $2\kappa\xi_1 + \Delta_1^\pm = 0$. For $b \sin(\varphi_1) > 0$ and $b \sin(\varphi_1) < 0$, u_1^\pm can, respectively, represent an exponential antidark (EAD) soliton on top of the cw background $u = \rho e^{2i\rho^2 t + i\phi}$ and an exponential dark (ED) soliton beneath the same background.

- (ii) If $\bar{\xi}_1 = -x + 2b\rho t = O(1)$, from $\xi_1 = -\bar{\xi}_1 + 4b\rho t$ we also have $\xi_1 \rightarrow \pm\infty$ as $\text{sgn}(b)t \rightarrow \pm\infty$. Then, calculating the limit of solution (16) when $\xi_1 \rightarrow \pm\infty$ gives another asymptotic expression in the exponential form

$$u \rightarrow \begin{cases} u_2^+ = \rho e^{2i\rho^2 t + i\phi} \left[1 - \frac{i(1 + e^{2i\theta})}{b r_1 e^{-2\kappa\bar{\xi}_1 - i(\theta + \varphi_1)} + i} \right] & (\text{sgn}(b)t \rightarrow \infty), \\ u_2^- = \rho e^{2i\rho^2 t + i\phi} \left[1 + \frac{i(1 + e^{-2i\theta})}{b r_1^{-1} e^{2\kappa\bar{\xi}_1 + i(\theta + \varphi_1)} - i} \right] & (\text{sgn}(b)t \rightarrow -\infty), \end{cases} \quad (20a)$$

$$|u| \rightarrow |u_2^\pm| = \rho \left[1 + \frac{2\sqrt{1 - b^2} \sin(2\theta + \varphi_1)}{\text{sgn}(b) \cosh(-2\kappa\bar{\xi}_1 - \Delta_1^\pm) - \sin(\theta + \varphi_1)} \right]^{\frac{1}{2}}. \quad (20b)$$

When condition (19) is satisfied, u_2^\pm is also nonsingular and is located in the line $2\kappa\bar{\xi}_1 + \Delta_1^\pm = 0$. Likewise, u_2^\pm can display the EAD and ED soliton profiles which are associated with $b \sin(2\theta + \varphi_1) > 0$ and $b \sin(2\theta + \varphi_1) < 0$, respectively.

- (iii) If $\eta_1 = x + 2\sigma\rho t = O(1)$, from $\xi_1 = \eta_1 + 2(b - \sigma)\rho t$ and $\bar{\xi}_1 = -\eta_1 + 2(b + \sigma)\rho t$ we know that $\xi_1 \rightarrow \mp\infty$ and $\bar{\xi}_1 \rightarrow \pm\infty$ as $\sigma t \rightarrow \pm\infty$. Then, by taking the limit of of solution (16) when $\xi_1, -\bar{\xi}_1 \rightarrow -\infty$ and $\xi_1, -\bar{\xi}_1 \rightarrow \infty$, we have the following asymptotic expression in the rational form

$$u \rightarrow u_3^\pm = \rho e^{2i\rho^2 t + i\phi} \left[1 + \frac{2\sigma}{2i\rho(\eta_1 + \gamma_2) - \sigma \pm 2i \sec(\theta)} \right] \quad (\sigma t \rightarrow \pm\infty), \quad (21a)$$

$$|u| \rightarrow |u_3^\pm| = \rho \left\{ 1 - \frac{8\rho\sigma\gamma_{2I}}{4[\rho\eta_1 + \rho\gamma_{2R} \pm \sec(\theta)]^2 + (2\rho\gamma_{2I} + \sigma)^2} \right\}^{\frac{1}{2}}. \quad (21b)$$

Apparently, u_3^\pm has no singularity if and only if

$$2\rho\gamma_{2I} + \sigma \neq 0, \quad (22)$$

and it can describe an rational antidark (RAD) soliton for $\sigma\gamma_{2I} < 0$ or an rational dark (RD) soliton for $\sigma\gamma_{2I} > 0$ in the line $\eta_1 + \gamma_{2R} \pm \frac{\sec(\theta)}{\rho} = 0$.

- (iv) If $\bar{\eta}_1 = -x + 2\sigma\rho t = O(1)$, from $\xi_1 = -\bar{\eta}_1 + 2(b + \sigma)\rho t$ and $\bar{\xi}_1 = \bar{\eta}_1 + 2(b - \sigma)\rho t$ we have $\xi_1 \rightarrow \pm\infty$ and $\bar{\xi}_1 \rightarrow \mp\infty$ as $\sigma t \rightarrow \pm\infty$. Then, by taking the limit of of solution (16) when $\xi_1, -\bar{\xi}_1 \rightarrow \infty$ and $\xi_1, -\bar{\xi}_1 \rightarrow -\infty$, we obtain another asymptotic expression in the rational form

$$u \rightarrow u_4^\pm = \rho e^{2i\rho^2 t + i\phi} \left[1 + \frac{2\sigma}{2i\rho(\bar{\eta}_1 + \gamma_{2R}^*) + \sigma \pm 2i\sec(\theta)} \right] \quad (\sigma t \rightarrow \pm\infty), \quad (23a)$$

$$|u| \rightarrow |u_4^\pm| = \rho^2 \left\{ 1 + \frac{8(1 + \rho\sigma\gamma_{2I})}{4[-\rho\bar{\eta}_1 - \rho\gamma_{2R} \mp \sec(\theta)]^2 + (2\rho\gamma_{2I} + \sigma)^2} \right\}^{\frac{1}{2}}. \quad (23b)$$

When condition (22) is satisfied, u_4^\pm is also nonsingular and it can represent an RAD soliton for $\sigma\gamma_{2I} > -\frac{1}{\rho}$ or an RD soliton for $\sigma\gamma_{2I} < -\frac{1}{\rho}$ in the line $\bar{\eta}_1 + \gamma_{2R} \pm \frac{\sec(\theta)}{\rho} = 0$.

3.2 Properties of soliton interactions

As shown in the above asymptotic analysis, solution (16) admits four pairs of asymptotic solitons (u_i^+, u_i^-) ($1 \leq i \leq 4$) which are localized in four different directions in the xt plane. Below, based on Eqs. (18a)–(23b), we further reveal the soliton interaction properties described by solution (16):

- (i) For each pair of asymptotic solitons (u_i^+, u_i^-), their intensities have the same amplitudes (i.e., $|u_i^\pm|_{\max}^2 - \rho^2$ for the antidark soliton or $\rho^2 - |u_i^\pm|_{\min}^2$ for the dark soliton):

$$A_1^\pm = \frac{2\rho^2\sqrt{1-b^2}|\sin(\varphi_1)|}{1 - \text{sgn}(b)\sin(\theta + \varphi_1)}, \quad A_2^\pm = \frac{2\rho^2\sqrt{1-b^2}|\sin(2\theta + \varphi_1)|}{1 - \text{sgn}(b)\sin(\theta + \varphi_1)}, \quad (24a)$$

$$A_3^\pm = \frac{8\rho^3|\gamma_{2I}|}{(1 + 2\rho\sigma\gamma_{2I})^2}, \quad A_4^\pm = \frac{8\rho^2|1 + \sigma\rho\gamma_{2I}|}{(1 + 2\sigma\rho\gamma_{2I})^2}. \quad (24b)$$

- (ii) The envelope velocity of u_i^+ is exactly equal to that of u_i^- , i.e.,

$$v_1^+ = v_1^- = -2\rho b, \quad v_2^+ = v_2^- = 2\rho b, \quad v_3^+ = v_3^- = 2\sigma\rho, \quad v_4^+ = v_4^- = -2\sigma\rho. \quad (25)$$

- (iii) All the exponential and rational solitons undergo the phase shifts for their envelopes and the phase differences can be given by

$$\delta\phi_1 = -\delta\phi_2 = \Delta_1^+ - \Delta_1^- = -2\ln|b|, \quad \delta\phi_3 = -\delta\phi_4 = 2\sec(\theta), \quad (26)$$

which is contrast to that there is no phase shift in the rational soliton solutions [15].

Therefore, all the interacting solitons can retain their individual shapes, amplitudes and velocities upon their mutual interactions except for some phase shift, which meets the nature of elastic soliton interactions.

Recalling that each pair of asymptotic solitons (u_i^+, u_i^-) ($1 \leq i \leq 4$) in solution (16) could be of the dark or antidark type, one can obtain a large variety of elastic soliton interactions. To illustrate, Figs. 1(a)–1(f) present some examples of four-soliton interactions. In particular, some soliton pair(s) (u_i^+, u_i^-) will vanish (i.e., the amplitude of $|u_i^\pm|^2$ becomes zero), and the relevant parametric condition is $\sin(\varphi_1) = 0$ for $i = 1$, $\sin(2\theta + \varphi_1) = 0$ for $i = 2$, $\gamma_{2I} = 0$ for $i = 3$, and $\sigma\gamma_{2I} = -\frac{1}{\rho}$ for $i = 4$. For those particular cases, the four-soliton interaction degenerates to a three-soliton interaction or even to a two-soliton interaction, as shown in Figs. 2(a)–2(e). However, the degenerate four-soliton interactions cannot be simply regarded as the conventional three- or two-soliton interactions since there are still the trace for the vanishing asymptotic soliton(s) in the near-field region (see Figs. 2(a)–2(e)). In Tables 1 and 2, we list all the possible cases of the exponential and rational asymptotic solitons and their related parametric conditions. The combinatorial calculation indicates that solution (16) can describe a total of forty different types of soliton interactions.

Table 1: Types of the exponential asymptotic solitons u_1^\pm and u_2^\pm with different parametric conditions.

Parametric conditions	Asymptotic soliton u_1^\pm [sgn(b) $t \rightarrow \pm\infty$]	Asymptotic soliton u_2^\pm [sgn(b) $t \rightarrow \pm\infty$]
$b \sin(\varphi_1) > 0, b \sin(2\theta + \varphi_1) > 0$	EAD soliton	EAD soliton
$b \sin(\varphi_1) > 0, b \sin(2\theta + \varphi_1) < 0$	EAD soliton	ED soliton
$b \sin(\varphi_1) < 0, b \sin(2\theta + \varphi_1) > 0$	ED soliton	EAD soliton
$b \sin(\varphi_1) < 0, b \sin(2\theta + \varphi_1) < 0$	ED soliton	ED soliton
$b \sin(\varphi_1) > 0, \sin(2\theta + \varphi_1) = 0$	EAD soliton	Vanish
$b \sin(\varphi_1) < 0, \sin(2\theta + \varphi_1) = 0$	ED soliton	Vanish
$\sin(\varphi_1) = 0, b \sin(2\theta + \varphi_1) > 0$	Vanish	EAD soliton
$\sin(\varphi_1) = 0, b \sin(2\theta + \varphi_1) < 0$	Vanish	ED soliton

4 The second type of mixed soliton solution

In this section, we consider that both λ_1 and λ_2 degenerate to $i b\rho$ with $0 < |b| < 1$. For simplicity, we set $\epsilon_1 = \epsilon_2 = \delta^2$ and $\lambda_1 = \lambda_2 = i\sigma\rho(1 + \delta^2)$, and take

$$\alpha_{1,2} = \alpha'_1 e^{h_1(s_1 + s_2 \delta^2)}, \quad \beta_{1,2} = \beta'_1 e^{-h_1(s_1 + s_2 \delta^2)}, \quad (27)$$

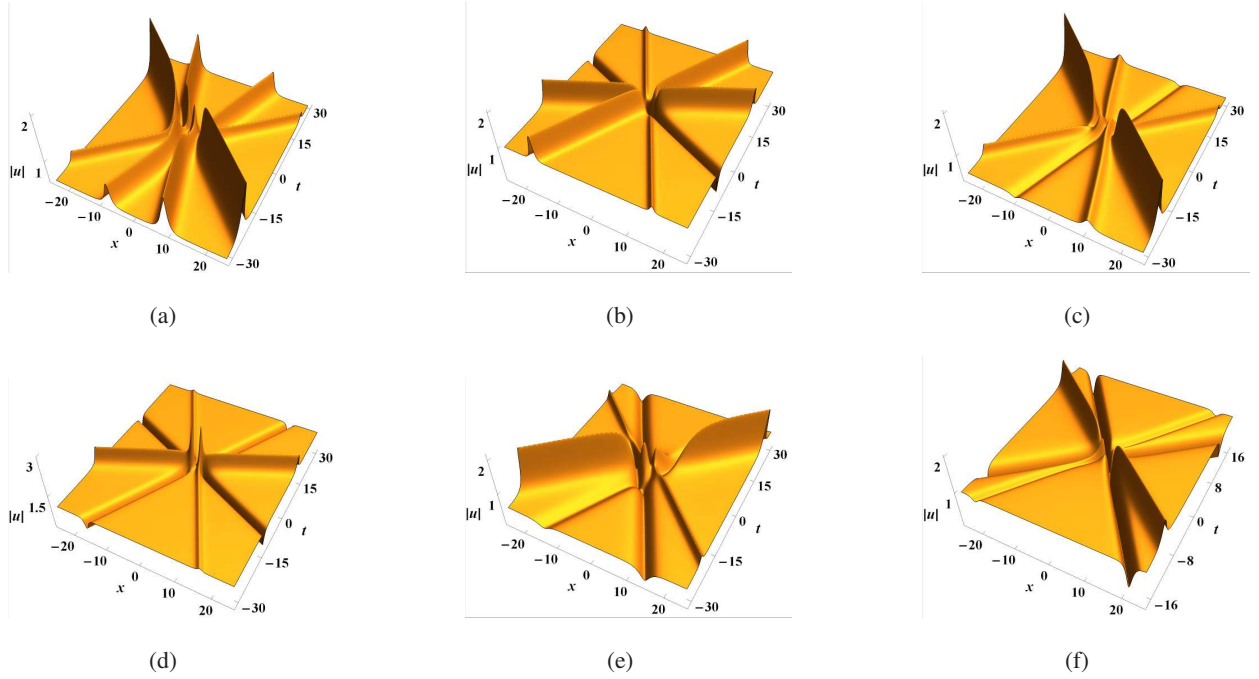


Figure 1: Six types of non-degenerate four-soliton interactions via solution (16): (a) EAD-EAD-RAD-RAD soliton interaction with $\rho = \frac{1}{2}$, $b = \frac{3}{10}$, $\phi = 0$, $\sigma = -1$, $\gamma_1 = -\frac{1}{20} + \frac{1}{10}i$ and $\gamma_2 = \frac{1}{5}i$; (b) EAD-EAD-RD-RAD soliton interaction with $\rho = 1$, $b = \frac{1}{4}$, $\phi = 0$, $\sigma = 1$, $\gamma_1 = 1 + \frac{1}{8}i$ and $\gamma_2 = i$; (c) EAD-ED-RAD-RAD soliton interaction with $\rho = \frac{1}{2}$, $b = \frac{3}{10}$, $\phi = 0$, $\sigma = -1$, $\gamma_1 = -1 + \frac{1}{2}i$ and $\gamma_2 = \frac{1}{5}i$; (d) EAD-ED-RD-RAD soliton interaction with $\rho = 1$, $b = \frac{1}{4}$, $\phi = 0$, $\sigma = 1$, $\gamma_1 = -1 + \frac{1}{8}i$ and $\gamma_2 = i$; (e) ED-ED-RAD-RAD soliton interaction with $\rho = \frac{1}{2}$, $b = \frac{1}{2}$, $\phi = 0$, $\sigma = 1$, $\gamma_1 = -\frac{1}{5}i$ and $\gamma_2 = -\frac{1}{5}i$; (f) ED-ED-RAD-RD soliton interaction with $\rho = 1$, $b = \frac{3}{5}$, $\phi = 0$, $\sigma = 1$, $\gamma_1 = -2i$ and $\gamma_2 = -2i$.

where $|\delta| \ll 1$ is a small parameter, and s_1 and s_2 are two arbitrary complex numbers. Based on the generalized DT, we must expand f_k and g_k ($k = 1, 2$) at $\lambda_{1,2} = i b \rho$ in the way of Eqs. (12) and (13) up to $j = 1$. Then, the second type of mixed soliton solution can be obtained as follows:

$$u = \rho e^{2i\rho^2 t + i\phi} + 2 \frac{\begin{vmatrix} f_1^{(0,0)} & f_1^{(1,0)} & f_1^{(2,0)} & g_1^{(0,0)} \\ f_1^{(0,1)} & f_1^{(1,1)} & f_1^{(2,1)} & g_1^{(0,1)} \\ -\bar{g}_1^{(0,0)} & -\bar{g}_1^{(1,0)} & -\bar{g}_1^{(2,0)} & \bar{f}_1^{(0,0)} \\ -\bar{g}_1^{(0,1)} & -\bar{g}_1^{(1,1)} & -\bar{g}_1^{(2,1)} & \bar{f}_1^{(0,1)} \end{vmatrix}}{\begin{vmatrix} f_1^{(0,0)} & f_1^{(1,0)} & g_1^{(0,0)} & -g_1^{(1,0)} \\ f_1^{(0,1)} & f_1^{(1,1)} & g_1^{(0,1)} & -g_1^{(1,1)} \\ -\bar{g}_1^{(0,0)} & -\bar{g}_1^{(1,0)} & \bar{f}_1^{(0,0)} & -\bar{f}_1^{(1,0)} \\ -\bar{g}_1^{(0,1)} & -\bar{g}_1^{(1,1)} & \bar{f}_1^{(0,1)} & -\bar{f}_1^{(1,1)} \end{vmatrix}}, \quad (28)$$

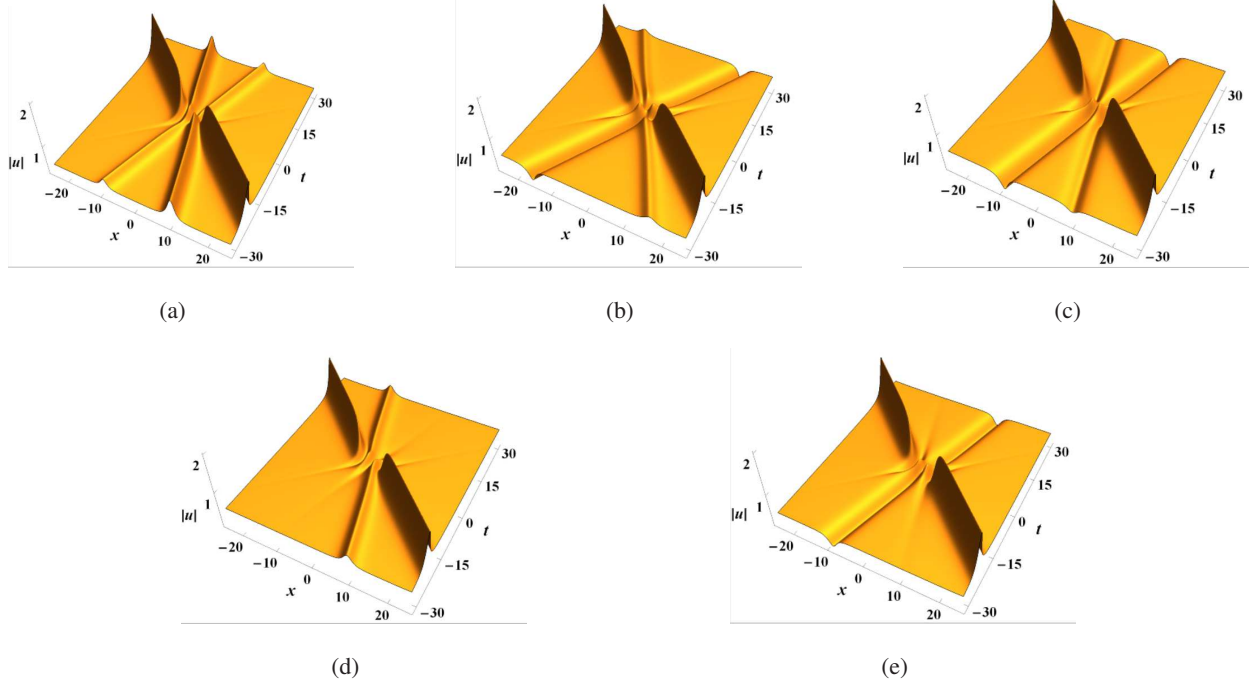


Figure 2: Five types of degenerate four-soliton interactions via solution (16): (a) EAD-EAD-V-RAD soliton interaction with $\rho = \frac{1}{2}$, $b = \frac{1}{4}$, $\phi = 0$, $\sigma = -1$, $\gamma_1 = -1 + i$ and $\gamma_2 = 0$. (b) EAD-ED-V-RAD soliton interaction with $\rho = \frac{1}{2}$, $b = \frac{1}{2}$, $\phi = 0$, $\sigma = -1$, $\gamma_1 = -1 + \frac{1}{2}i$ and $\gamma_2 = 0$. (c) ED-ED-V-RAD soliton interaction with $\rho = \frac{1}{2}$, $b = \frac{1}{4}$, $\phi = 0$, $\sigma = -1$, $\gamma_1 = -1 - \frac{1}{2}i$ and $\gamma_2 = 0$. (d) EAD-V-V-RAD soliton interaction with $\rho = \frac{1}{2}$, $b = \frac{1}{4}$, $\phi = 0$, $\sigma = -1$, $\gamma_1 = -\frac{7}{2\sqrt{15}} + \frac{1}{2}i$ and $\gamma_2 = 0$. (e) V-ED-V-RAD soliton interaction with $\rho = \frac{1}{2}$, $b = \frac{1}{4}$, $\phi = 0$, $\sigma = -1$, $\gamma_1 = -1$ and $\gamma_2 = 0$. Here, “V” represents the vanishment of an asymptotic soliton as $|t| \rightarrow \infty$.

with

$$f_1^{(0,0)} = \alpha'_1 e^{i\rho^2 t + \frac{i\phi}{2}} (e^{\kappa(\xi_1 + s_1)} + \gamma_1 e^{-\kappa(\xi_1 + s_1)}), \quad (29a)$$

$$f_1^{(0,1)} = -\frac{\alpha'_1 \rho \chi(x, t)}{\sqrt{1 - b^2}} e^{i\rho^2 t + \frac{i\phi}{2}} (e^{\kappa(\xi_1 + s_1)} - \gamma_1 e^{-\kappa(\xi_1 + s_1)}), \quad (29b)$$

$$f_1^{(k,0)} = (i\rho b)^k f_1^{(0,0)}, \quad f_1^{(k,1)} = (i\rho b)^k f_1^{(0,1)} + k f_1^{(k,0)} \quad (k = 1, 2), \quad (29c)$$

$$g_1^{(0,0)} = \alpha'_1 e^{-i\rho^2 t - \frac{i\phi}{2}} (e^{\kappa(\xi_1 + s_1) - i\theta} - \gamma_1 e^{-\kappa(\xi_1 + s_1) + i\theta}), \quad (29d)$$

$$g_1^{(0,1)} = \frac{-\alpha'_1 [\rho \chi(x, t) + ib]}{\sqrt{1 - b^2}} e^{-i\rho^2 t - \frac{i\phi}{2}} (e^{\kappa(\xi_1 + s_1) - i\theta} + \gamma_1 e^{-\kappa(\xi_1 + s_1) + i\theta}), \quad (29e)$$

$$g_1^{(k,0)} = (i\rho b)^k g_1^{(0,0)}, \quad g_1^{(k,1)} = (i\rho b)^k g_1^{(0,1)} + k g_1^{(k,0)} \quad (k = 1, 2), \quad (29f)$$

$$\chi(x, t) = (b^2 - 1)(2b\rho t + s_2) + b^2(\xi_1 + s_1), \quad \xi_1 = x + 2b\rho t, \quad (29g)$$

$$\kappa = \rho\sqrt{1 - b^2}, \quad \theta = \arctan(b/\sqrt{1 - b^2}), \quad \gamma_1 = \beta'_1/\alpha'_1 = r_1 e^{i\varphi_1}, \quad (29h)$$

Table 2: Types of the rational asymptotic solitons u_3^\pm and u_4^\pm with different parametric conditions.

Parametric conditions	Asymptotic soliton u_3^\pm ($\sigma t \rightarrow \pm\infty$)	Asymptotic soliton u_4^\pm ($\sigma t \rightarrow \pm\infty$)
$\sigma\gamma_{2I} < -\frac{1}{\rho}$	RAD soliton	RD soliton
$-\frac{1}{\rho} < \sigma\gamma_{2I} < 0$	RAD soliton	RAD soliton
$\sigma\gamma_{2I} > 0$	RD soliton	RAD soliton
$\gamma_{2I} = 0$	Vanish	RAD soliton
$\sigma\gamma_{2I} = -\frac{1}{\rho}$	RAD soliton	Vanish

where $-\pi/2 < \theta < \pi/2$, $-\pi < \varphi_1 < \pi$, $r_1 > 0$ is a real constant, the *bar* denotes the combination of complex conjugate and space reversal, and α'_1 will be canceled out when Eqs. (29a)–(29h) are substituted into Eq. (28). Also, this solution is in the mixed exponential-rational form since it includes both the exponential terms $e^{\pm\kappa\xi_1}$, $e^{\pm\kappa\bar{\xi}_1}$ and algebraic terms $\chi(x, t)$, $\bar{\chi}(x, t)$. In the following, we will develop the asymptotic analysis method so as to understand the solitonic behavior in solution (28).

4.1 Asymptotic analysis

To begin with, we argue that the asymptotic solitons of solution (28) cannot be located in any straight line $x - ct' = \text{const}$ with $t' = \text{sgn}(b)t$. Noticing that $\xi_1 - (x - ct') = (c + 2|b|\rho)t'$ and $-\bar{\xi}_1 - (x - ct') = (c - 2|b|\rho)t'$, we have the asymptotic behavior of ξ_1 and $-\bar{\xi}_1$ when $t' \rightarrow \pm\infty$:

$$\xi_1 \rightarrow \begin{cases} \pm\infty, & c > -2|b|\rho, \\ O(1), & c = -2|b|\rho, \\ \mp\infty, & c < -2|b|\rho, \end{cases} \quad \bar{\xi}_1 \rightarrow \begin{cases} \mp\infty, & c > 2|b|\rho, \\ O(1), & c = 2|b|\rho, \\ \pm\infty, & c < 2|b|\rho. \end{cases} \quad (30)$$

Thus, no matter whether c is equal to $\pm 2|b|\rho$ or not, the limit of solution (28) along the line $x - ct' = \text{const}$ as $t' \rightarrow \pm\infty$ is a plane wave, that is,

$$\lim_{t' \rightarrow \pm\infty} u = \begin{cases} \rho e^{2i\rho^2 t + i\phi} & (|c| > 2|b|\rho), \\ \rho e^{2i\rho^2 t + i\phi \pm 4i\theta} & (-2|b|\rho < c < 2|b|\rho), \\ -\rho e^{2i\rho^2 t + i\phi \pm 2i\theta} & (c = \pm 2|b|\rho), \end{cases} \quad (31)$$

which implies that there is no asymptotic soliton lying in any straight line of the xt plane.

Next, we consider that the asymptotic solitons of solution (28) are located in some curves $F(x, t') = 0$. Because $-\frac{F_{t'}}{F_x} \neq \text{const}$, both ξ_1 and $\bar{\xi}_1$ will tend to $+\infty$ or $-\infty$ along $F(x, t') = 0$ as $t' \rightarrow \infty$. Thus, before

explicitly determining the curves $F(x, t') = 0$, one can calculate the *intermediate* asymptotic expressions of solution (28) by letting $\bar{\xi}_1 \rightarrow \pm\infty$ or $\xi_1 \rightarrow \pm\infty$. If precedly taking $\bar{\xi}_1 \rightarrow \pm\infty$ for solution (28), we have the limits as follows:

$$u \rightarrow u_I = \rho e^{2i\rho^2 t + i\phi} \times \left\{ 1 + \frac{4b\sqrt{1-b^2}[e^{2\kappa(\xi_1+s_1)} + \gamma_1(1 + \sqrt{1-b^2}\zeta)]}{\omega e^{2\kappa(\xi_1+s_1)} - 2b\sqrt{1-b^2}\gamma_1(1 + \zeta e^{-i\theta}) - ib^4\gamma_1^2 e^{-2\kappa(\xi_1+s_1)}} \right\} \quad (\bar{\xi}_1 \rightarrow +\infty), \quad (32)$$

$$u \rightarrow u_{II} = \rho e^{2i\rho^2 t + i\phi} \times \left\{ 1 + \frac{4b\sqrt{1-b^2}[\gamma_1 e^{2\kappa(\xi_1+s_1)}(1 - \sqrt{1-b^2}\zeta) + \gamma_1^2]}{ib^4 e^{4\kappa(\xi_1+s_1)} - 2b\sqrt{1-b^2}\gamma_1 e^{2\kappa(\xi_1+s_1)}(1 - \zeta e^{i\theta}) + \omega^* \gamma_1^2} \right\} \quad (\bar{\xi}_1 \rightarrow -\infty), \quad (33)$$

with $\omega = -ie^{-2i\theta}$ and $\zeta = 2\rho[b^2(\xi_1 + s_1 + s_2) - s_2] - 4\rho^2|b|(1-b^2)t'$. Here, both Eqs. (32) and (33) contain two independent variables ξ_1 and t' , so that the soliton center trajectories cannot be directly obtained by calculating the extreme values of $|u_I|^2$ and $|u_{II}|^2$.

In fact, there must be some balance between ξ_1 and t' in Eqs. (32) and (33) when an asymptotic soliton appears as $t' \rightarrow \pm\infty$. By the method of dominant balance [42], we assume that

$$t' \sim W(x, t)(e^{2\kappa\xi_1})^p, \quad W(x, t) = O(1), \quad (34)$$

where p is a constant to be determined. It can be found that as $t' \rightarrow \pm\infty$ both Eqs. (32) and (33) approaches a plane wave as given in Eq. (31) for all the cases when $p \neq \pm 1$. Therefore, Eq. (34) with $p = \pm 1$ is the only allowed balance for deriving the asymptotic solitons from Eqs. (32) and (33). With an elaborate computation on Mathematica, we obtain that there are four asymptotic solitons in the mixed exponential-rational form:

(i) If $W(x, t) = t'e^{-2\kappa\xi_1} = O(1)$, we take the limit of u_I when $\xi_1 \rightarrow +\infty$, yielding

$$u_I \rightarrow u_1^+ = \rho e^{2i\rho^2 t + i\phi} \left\{ 1 + \frac{4b\sqrt{1-b^2}\omega^*[1 - 4\rho^2\gamma_1 b(1-b^2)^{\frac{3}{2}} t e^{-2\kappa(\xi_1+s_1)}]}{1 + 8i\rho^2\gamma_1 b^2(1-b^2)^{\frac{3}{2}} e^{i\theta} t e^{-2\kappa(\xi_1+s_1)}} \right\}, \quad (35a)$$

$$|u_I| \rightarrow |u_1^+| = \rho \left[1 + \frac{2\sqrt{1-b^2} \sin(\varphi_1 - 2\kappa s_{1I})}{\text{sgn}(b) \cosh(2\kappa\xi_1 + 2\kappa s_{1R} - \ln \Xi_1^+) - \sin(\theta + \varphi_1 - 2\kappa s_{1I})} \right]^{\frac{1}{2}}, \quad (35b)$$

with $\Xi_1^+ = 8\rho^2 r_1 b^2 (1-b^2)^{\frac{3}{2}} t'$. When φ_1 , b and s_1 satisfy

$$\theta + \varphi_1 - 2\kappa s_{1I} \neq 2k\pi + \frac{1}{2}\text{sgn}(b)\pi \quad (k \in \mathbb{Z}), \quad (36)$$

u_1^+ is nonsingular and it can represent an mixed antidark (MAD) soliton for $\text{sgn}(b) \sin(\varphi_1 - 2\kappa s_{1I}) > 0$ or an mixed dark (MD) soliton for $\text{sgn}(b) \sin(\varphi_1 - 2\kappa s_{1I}) < 0$. Note that the asymptotic expression (35a) is obtained by orderly letting $\bar{\xi}_1, \xi_1 \rightarrow +\infty$. Since $\xi_1 + \bar{\xi}_1 = 4\rho|b|t' \rightarrow +\infty$, u_1^+ appears

as an asymptotic state of solution (28) as $t' \rightarrow +\infty$. Meanwhile, calculating the extreme value of $|u_1^+|^2$ shows that the soliton center trajectory is

$$\mathcal{C}_1^+ : t' e^{-\kappa \xi_1} = \frac{e^{2\kappa s_{1R}}}{8\rho^2 r_1 b^2 (1-b^2)^{\frac{3}{2}}} \quad (t' > 0), \quad (37)$$

where its slope is given by

$$K_1^+ = -\frac{1}{2|b|\rho} + \frac{1}{2|b|\rho - 8\rho^3 b^2 \sqrt{1-b^2} t'}. \quad (38)$$

Observing that $K_1^+ < -\frac{1}{2|b|\rho}$ when $t' > \frac{1}{4\rho^2 |b| \sqrt{1-b^2}}$, we know that the asymptotic soliton u_1^+ lies in the region between the direction $l_1 : t' = -\frac{1}{2|b|\rho} x$ and positive t' -axis, as seen in Fig. 3.

(ii) If $W(x, t) = t' e^{2\kappa \xi_1} = O(1)$, we take the limit of u_{II} when $\xi_1 \rightarrow -\infty$, yielding

$$u_{\text{II}} \rightarrow u_1^- = \rho e^{2i\rho^2 t + i\phi} \left\{ 1 + \frac{4b\sqrt{1-b^2}\omega [\gamma_1 + 4\rho^2 b(1-b^2)^{\frac{3}{2}} t e^{2\kappa(\xi_1 + s_1)}]}{\gamma_1 + 8i\rho^2 b^2 (1-b^2)^{\frac{3}{2}} e^{-i\theta} t e^{2\kappa(\xi_1 + s_1)}} \right\}, \quad (39a)$$

$$|u_{\text{II}}| \rightarrow |u_1^-| = \rho \left[1 + \frac{2\sqrt{1-b^2} \sin(\varphi_1 - 2\kappa s_{1I})}{\text{sgn}(b) \cosh(2\kappa \xi_1 + 2\kappa s_{1R} + \ln \Xi_1^-) - \sin(\theta + \varphi_1 - 2\kappa s_{1I})} \right]^{\frac{1}{2}}, \quad (39b)$$

with $\Xi_1^- = -8\rho^2 b^2 (1-b^2)^{\frac{3}{2}} t' / r_1$. When condition (36) is satisfied, u_1^- is also nonsingular and it can represent an MAD soliton for $\text{sgn}(b) \sin(\varphi_1 - 2\kappa s_{1I}) > 0$ or an MD soliton for $\text{sgn}(b) \sin(\varphi_1 - 2\kappa s_{1I}) < 0$. Since the asymptotic expression (39a) is obtained by orderly letting $\bar{\xi}_1, \xi_1 \rightarrow -\infty$, one immediately has $\xi_1 + \bar{\xi}_1 = 4\rho |b| t' \rightarrow -\infty$. That is, u_1^- appears as an asymptotic state of solution (28) as $t' \rightarrow -\infty$. Via the extreme value analysis, the soliton center trajectory of u_1^- can be determined as

$$\mathcal{C}_1^- : t' e^{\kappa \xi_1} = -\frac{r_1 e^{-2\kappa s_{1R}}}{8\rho^2 b^2 (1-b^2)^{\frac{3}{2}}} \quad (t' < 0), \quad (40)$$

and its slope is given by

$$K_1^- = -\frac{1}{2|b|\rho} + \frac{1}{2|b|\rho + 8\rho^3 b^2 \sqrt{1-b^2} t'}, \quad (41)$$

which implies that $K_1^- < -\frac{1}{2|b|\rho}$ when $t' < -\frac{1}{4\rho^2 |b| \sqrt{1-b^2}}$. Therefore, the asymptotic soliton u_1^- is located in the region between the direction l_1 and negative t' -axis, as seen in Fig. 3.

(iii) If $W(x, t) = t' e^{2\kappa \xi_1} = O(1)$, we take the limit of u_{I} when $\xi_1 \rightarrow -\infty$, yielding

$$u_{\text{I}} \rightarrow u_2^+ = \rho e^{2i\rho^2 t + i\phi} \left[1 - \frac{16\rho^2 (1-b^2)^2 t e^{2\kappa(\xi_1 + s_1)}}{8\rho^2 (1-b^2)^{\frac{3}{2}} e^{-i\theta} t e^{2\kappa(\xi_1 + s_1)} - i b^2 \gamma_1} \right], \quad (42a)$$

$$|u_{\text{I}}| \rightarrow |u_2^+| = \rho \left[1 - \frac{2\sqrt{1-b^2} \sin(\varphi_1 - 2\kappa s_{1I})}{\text{sgn}(b) \cosh(2\kappa \xi_1 + 2\kappa s_{1R} + \ln \Xi_2^+) + \sin(\theta + \varphi_1 - 2\kappa s_{1I})} \right]^{\frac{1}{2}}, \quad (42b)$$

with $\Xi_2^+ = 8\rho^2(1-b^2)^{\frac{3}{2}}t'/(b^2r_1)$. When φ_1 , b and s_1 satisfy

$$\theta + \varphi_1 - 2\kappa s_{1I} \neq 2k\pi - \frac{1}{2}\text{sgn}(b)\pi \quad (k \in \mathbb{Z}), \quad (43)$$

u_2^+ is nonsingular and it can represent an MAD soliton for $\text{sgn}(b)\sin(\varphi_1 - 2\kappa s_{1I}) < 0$ or an MD soliton for $\text{sgn}(b)\sin(\varphi_1 - 2\kappa s_{1I}) > 0$. Note that the asymptotic expression (42a) is obtained by orderly letting $\bar{\xi}_1 \rightarrow +\infty$ and $\xi_1 \rightarrow -\infty$, which implies that $(\xi_1 - \bar{\xi}_1)/2 = x \rightarrow -\infty$. Meanwhile, calculation of the extreme value of $|u_2^+|^2$ shows that the soliton center trajectory is

$$C_2^+ : t'e^{\kappa\xi_1} = \frac{b^2r_1e^{-2\kappa s_{1R}}}{8\rho^2(1-b^2)^{\frac{3}{2}}} \quad (t' > 0), \quad (44)$$

where its slope is given by

$$K_2^+ = -\frac{1}{2|b|\rho} + \frac{1}{2|b|\rho + 8\rho^3b^2\sqrt{1-b^2}t'}. \quad (45)$$

Noticing that $-\frac{1}{2|b|\rho} < K_2^+ < 0$ for $t' > 0$ and $K_2^+ < -\frac{1}{2|b|\rho}$ when $t' < \frac{-1}{4\rho^2|b|\sqrt{1-b^2}}$, we know that u_2^+ must appear as an asymptotic soliton of solution (28) as $t' \rightarrow +\infty$, and it is located in the region between the direction l_1 and negative x -axis, as seen in Fig. 3.

(iv) If $W(x, t) = t'e^{-2\kappa\xi_1} = O(1)$, we take the limit of u_{II} when $\xi_1 \rightarrow +\infty$, yielding

$$u_{\text{II}} \rightarrow u_2^- = \rho e^{2i\rho^2t+i\phi} \left[1 - \frac{16\rho^2(1-b^2)^2\gamma_1 t e^{-2\kappa(\xi_1+s_1)}}{8\rho^2(1-b^2)^{\frac{3}{2}}\gamma_1 e^{i\theta} t e^{-2\kappa(\xi_1+s_1)} - ib^2} \right], \quad (46a)$$

$$|u_{\text{II}}| \rightarrow |u_2^-| = \rho \left[1 - \frac{2\sqrt{1-b^2}\sin(\varphi_1 - 2\kappa s_{1I})}{\text{sgn}(b)\cosh(2\kappa\xi_1 + 2\kappa s_{1R} - \ln \Xi_2^-) + \sin(\theta + \varphi_1 - 2\kappa s_{1I})} \right]^{\frac{1}{2}}, \quad (46b)$$

with $\Xi_2^- = -8\rho^2(1-b^2)^{\frac{3}{2}}r_1t'/b^2$. When condition (43) is satisfied, u_2^- is also nonsingular and it can represent an MAD soliton for $\text{sgn}(b)\sin(\varphi_1 - 2\kappa s_{1I}) < 0$ or an MD soliton for $\text{sgn}(b)\sin(\varphi_1 - 2\kappa s_{1I}) > 0$. Since the asymptotic expression (46a) is obtained by orderly letting $\bar{\xi}_1 \rightarrow -\infty$ and $\xi_1 \rightarrow +\infty$, one immediately have $(\xi_1 - \bar{\xi}_1)/2 = x \rightarrow +\infty$. Via the extreme value analysis, the soliton center trajectory of u_2^- can be determined as

$$C_2^- : t'e^{-\kappa\xi_1} = -\frac{b^2e^{2\kappa s_{1R}}}{8\rho^2(1-b^2)^{\frac{3}{2}}r_1} \quad (t' < 0), \quad (47)$$

and its slope is given by

$$K_2^- = -\frac{1}{2|b|\rho} + \frac{1}{2|b|\rho - 8\rho^3b^2\sqrt{1-b^2}t'}, \quad (48)$$

which implies that $-\frac{1}{2\rho|b|} < K_2^- < 0$ for $t' < 0$ and $K_2^- < -\frac{1}{2\rho|b|}$ when $t' > \frac{1}{4\rho^2|b|\sqrt{1-b^2}}$. Therefore, u_2^- must appear as an asymptotic soliton of solution (28) as $t' \rightarrow -\infty$, and it is located in the region between the direction l_1 and positive x -axis, as seen in Fig. 3.

On the other hand, by precedly taking $\xi_1 \rightarrow \pm\infty$ for solution (28), we have another two *intermediate* asymptotic expressions:

$$u \rightarrow u_{\text{III}} = \rho e^{2i\rho^2 t + i\phi} \times \left\{ 1 + \frac{4b\sqrt{1-b^2} [\omega^* e^{2\kappa(\bar{\xi}_1 + s_1^*)} + i\gamma_1^* (2ib\sqrt{1-b^2} - \sqrt{1-b^2} \bar{\zeta} - 1)]}{e^{2\kappa(\bar{\xi}_1 + s_1^*)} + 2ib\sqrt{1-b^2} \gamma_1^* (e^{-2i\theta} + \bar{\zeta} e^{-i\theta}) + ib^4 \omega \gamma_1^{*2} e^{-2\kappa(\bar{\xi}_1 + s_1^*)}} \right\} \quad (\xi_1 \rightarrow \infty), \quad (49)$$

$$u \rightarrow u_{\text{IV}} = \rho e^{2i\rho^2 t + i\phi} \times \left\{ 1 + \frac{4b\sqrt{1-b^2} [\gamma_1^* e^{2\kappa(\bar{\xi}_1 + s_1^*)} (\sqrt{1-b^2} \bar{\zeta} - 2ib\sqrt{1-b^2} - 1) + i\omega \gamma_1^{*2}]}{\omega^* b^4 e^{4\kappa(\bar{\xi}_1 + s_1^*)} + 2b\sqrt{1-b^2} \gamma_1^* e^{2\kappa(\bar{\xi}_1 + s_1^*)} (e^{2i\theta} - \bar{\zeta} e^{i\theta}) + i\gamma_1^{*2}} \right\} \quad (\xi_1 \rightarrow -\infty), \quad (50)$$

with $\bar{\zeta} = 2\rho[b^2(\bar{\xi}_1 + s_1^* + s_2^*) - s_2^*] - 4\rho^2|b|(1-b^2)t'$. With an asymptotic analysis of Eqs. (49) and (50) like the above treatment on Eqs. (32) and (33), the other four mixed asymptotic solitons of solution (28) can be obtained as follows:

- (i) Taking the limit of u_{III} when $\bar{\xi}_1 \rightarrow +\infty$, the asymptotic expression along the curve $W(x, t) = t' e^{-2\kappa\bar{\xi}_1} = O(1)$ is given by

$$u_{\text{III}} \rightarrow u_3^+ = \rho e^{2i\rho^2 t + i\phi} \left\{ 1 + \frac{4b\sqrt{1-b^2} [i\omega^* - 4\rho^2 b(1-b^2)^{\frac{3}{2}} \gamma_1^* t e^{-2\kappa(\bar{\xi}_1 + s_1^*)}]}{i + 8\rho^2 b^2 (1-b^2)^{\frac{3}{2}} \gamma_1^* e^{-i\theta} t e^{-2\kappa(\bar{\xi}_1 + s_1^*)}} \right\}, \quad (51a)$$

$$|u_{\text{III}}| \rightarrow |u_3^+| = \rho \left[1 + \frac{2\sqrt{1-b^2} \sin(2\theta + \varphi_1 - 2\kappa s_{1I})}{\text{sgn}(b) \cosh(2\kappa\bar{\xi}_1 + 2\kappa s_{1R} - \ln \Xi_1^+) - \sin(\theta + \varphi_1 - 2\kappa s_{1I})} \right]^{\frac{1}{2}}, \quad (51b)$$

where the superscript “+” means $t' \rightarrow +\infty$.

- (ii) Taking the limit of u_{IV} when $\bar{\xi}_1 \rightarrow -\infty$, the asymptotic expression along the curve $W(x, t) = t' e^{2\kappa\bar{\xi}_1} = O(1)$ is given by

$$u_{\text{IV}} \rightarrow u_3^- = \rho e^{2i\rho^2 t + i\phi} \left\{ 1 + \frac{4b\sqrt{1-b^2} [i\omega \gamma_1^* - 4\rho^2 b(1-b^2)^{\frac{3}{2}} t e^{2\kappa(\bar{\xi}_1 + s_1^*)}]}{i\gamma_1^* + 8\rho^2 b^2 (1-b^2)^{\frac{3}{2}} e^{i\theta} t e^{2\kappa(\bar{\xi}_1 + s_1^*)}} \right\}, \quad (52a)$$

$$|u_{\text{IV}}| \rightarrow |u_3^-| = \rho \left[1 + \frac{2\sqrt{1-b^2} \sin(2\theta + \varphi_1 - 2\kappa s_{1I})}{\text{sgn}(b) \cosh(2\kappa\bar{\xi}_1 + 2\kappa s_{1R} + \ln \Xi_1^-) - \sin(\theta + \varphi_1 - 2\kappa s_{1I})} \right]^{\frac{1}{2}}, \quad (52b)$$

where the superscript “-” means $t' \rightarrow -\infty$.

- (iii) Taking the limit of u_{III} when $\bar{\xi}_1 \rightarrow -\infty$, the asymptotic expression along the curve $W(x, t) = t' e^{2\kappa\bar{\xi}_1} = O(1)$ is given by

$$u_{\text{III}} \rightarrow u_4^+ = \rho e^{2i\rho^2 t + i\phi} \left[1 - \frac{16\rho^2 (1-b^2)^2 t e^{2\kappa(\bar{\xi}_1 + s_1^*)}}{8\rho^2 (1-b^2)^{\frac{3}{2}} e^{-i\theta} t e^{2\kappa(\bar{\xi}_1 + s_1^*)} - b^2 \omega \gamma_1^*} \right], \quad (53a)$$

$$|u_{\text{III}}| \rightarrow |u_4^+| = \rho \left[1 - \frac{2\sqrt{1-b^2} \sin(2\theta + \varphi_1 - 2\kappa s_{1I})}{\text{sgn}(b) \cosh(2\kappa\bar{\xi}_1 + 2\kappa s_{1R} + \ln \Xi_2^+) + \sin(\theta + \varphi_1 - 2\kappa s_{1I})} \right]^{\frac{1}{2}}, \quad (53b)$$

where the superscript “+” means $t' \rightarrow +\infty$.

(iv) Taking the limit of u_{IV} when $\bar{\xi}_1 \rightarrow +\infty$, the asymptotic expression along the curve $W(x, t) = t'e^{-2\kappa\bar{\xi}_1} = O(1)$ is given by

$$u_{IV} \rightarrow u_4^- = \rho e^{2i\rho^2 t + i\phi} \left[1 - \frac{16\rho^2(1-b^2)^2 \gamma_1^* t e^{-2\kappa(\bar{\xi}_1 + s_1^*)}}{8\rho^2(1-b^2)^{\frac{3}{2}} \gamma_1^* e^{i\theta} t e^{-2\kappa(\bar{\xi}_1 + s_1^*)} + b^2 \omega^*} \right], \quad (54a)$$

$$|u_{IV}| \rightarrow |u_4^-| = \rho \left[1 - \frac{2\sqrt{1-b^2} \sin(2\theta + \varphi_1 - 2\kappa s_{1I})}{\text{sgn}(b) \cosh(2\kappa\bar{\xi}_1 + 2\kappa s_{1R} - \ln \Xi_2^-) + \sin(\theta + \varphi_1 - 2\kappa s_{1I})} \right]^{\frac{1}{2}}, \quad (54b)$$

where the superscript “-” means $t' \rightarrow -\infty$.

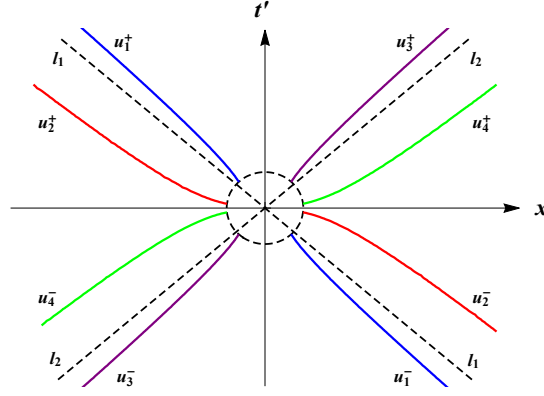


Figure 3: Schematic diagrams for the distribution of eight asymptotic solitons in solution (28), where the dashed oval stands for the soliton interaction region.

As seen from Eqs. (51a)–(54b), we know that u_3^\pm is nonsingular with condition (36) and it can describe an MAD soliton for $\text{sgn}(b) \sin(2\theta + \varphi_1 - 2\kappa s_{1I}) > 0$ or an MD soliton for $\text{sgn}(b) \sin(2\theta + \varphi_1 - 2\kappa s_{1I}) < 0$; u_4^\pm is nonsingular with condition (43) and it can describe an MAD soliton for $\text{sgn}(b) \sin(2\theta + \varphi_1 - 2\kappa s_{1I}) < 0$ or an MD soliton for $\text{sgn}(b) \sin(2\theta + \varphi_1 - 2\kappa s_{1I}) > 0$. Meanwhile, the center trajectories and their slopes of the asymptotic solitons u_3^\pm and u_4^\pm can be given as follows:

$$C_3^+ : t'e^{-2\kappa\bar{\xi}_1} = \frac{e^{2\kappa s_{1R}}}{8\rho^2 b^2 (1-b^2)^{\frac{3}{2}} r_1}, \quad K_3^+ = \frac{1}{2\rho|b|} - \frac{1}{2\rho|b| - 8\rho^3 b^2 \sqrt{1-b^2} t'}, \quad (55a)$$

$$C_3^- : t'e^{2\kappa\bar{\xi}_1} = -\frac{r_1 e^{-2\kappa s_{1R}}}{8\rho^2 b^2 (1-b^2)^{\frac{3}{2}}}, \quad K_3^- = \frac{1}{2\rho|b|} - \frac{1}{2\rho|b| + 8\rho^3 b^2 \sqrt{1-b^2} t'}, \quad (55b)$$

$$C_4^+ : t'e^{2\kappa\bar{\xi}_1} = \frac{b^2 r_1 e^{-2\kappa s_{1R}}}{8\rho^2 (1-b^2)^{\frac{3}{2}}}, \quad K_4^+ = \frac{1}{2\rho|b|} - \frac{1}{2\rho|b| + 8\rho^3 b^2 \sqrt{1-b^2} t'}, \quad (55c)$$

$$C_4^- : t'e^{-2\kappa\bar{\xi}_1} = -\frac{b^2 e^{2\kappa s_{1R}}}{8\rho^2 (1-b^2)^{\frac{3}{2}} r_1}, \quad K_4^- = \frac{1}{2\rho|b|} - \frac{1}{2\rho|b| - 8\rho^3 b^2 \sqrt{1-b^2} t'}. \quad (55d)$$

It can be readily obtained that the slope $K_3^+ > \frac{1}{2|b|\rho}$ when $t' > \frac{1}{4\rho^2|b|\sqrt{1-b^2}}$, $K_3^- > \frac{1}{2|b|\rho}$ when $t' < -\frac{1}{4\rho^2|b|\sqrt{1-b^2}}$, $0 < K_4^+ < \frac{1}{2|b|\rho}$ when $t' > 0$, and $0 < K_4^- < \frac{1}{2|b|\rho}$ when $t' < 0$. That is, the asymptotic

soliton u_3^+ is situated between the direction $l_2 : t' = \frac{1}{2|b|\rho}x$ and positive t' -axis, u_3^- is between the direction l_2 and negative t' -axis, u_4^+ is between the direction l_2 and positive x -axis, and u_4^- is between the direction l_2 and negative x -axis. The distribution of four asymptotic soliton pairs in the xt' plane can be found in Fig. 3.

The above asymptotic analysis of solution (28) is apparently more complicated than that of solution (16), and unconventionally the center trajectories of eight asymptotic solitons u_i^\pm ($1 \leq i \leq 4$) are all along some curved lines in the xt' plane. Naturally, one may ask how well those asymptotic expressions approximate the exact solution when $|t'| \gg 1$. In Fig. 4, we compare the asymptotic solitons u_i^\pm ($1 \leq i \leq 4$) with the exact solution (28) at different values of t' . The graphical comparison shows that the asymptotic expressions give a good approximation to solution (28) for large values of t' .

4.2 Properties of soliton interactions

Based on the obtained asymptotic expressions in Subsection 4.1, we discuss the soliton interaction properties of solution (28) in the following aspects:

- (i) By calculating the absolute differences between $|u_i^\pm|_{\max}^2$ and ρ^2 for the MAD solitons (or between $|u_i^\pm|_{\min}^2$ and ρ^2 for the MD solitons), we get the amplitudes for $|u_i^\pm|^2$ ($1 \leq i \leq 4$) as follows:

$$A_1^\pm = \frac{2\rho^2\sqrt{1-b^2}|\sin(\varphi_1 - 2\kappa s_{1I})|}{1 - \operatorname{sgn}(b)\sin(\theta + \varphi_1 - 2\kappa s_{1I})}, \quad A_2^\pm = \frac{2\rho^2\sqrt{1-b^2}|\sin(\varphi_1 - 2\kappa s_{1I})|}{1 + \operatorname{sgn}(b)\sin(\theta + \varphi_1 - 2\kappa s_{1I})}, \quad (56a)$$

$$A_3^\pm = \frac{2\rho^2\sqrt{1-b^2}|\sin(2\theta + \varphi_1 - 2\kappa s_{1I})|}{1 - \operatorname{sgn}(b)\sin(\theta + \varphi_1 - 2\kappa s_{1I})}, \quad A_4^\pm = \frac{2\rho^2\sqrt{1-b^2}|\sin(2\theta + \varphi_1 - 2\kappa s_{1I})|}{1 + \operatorname{sgn}(b)\sin(\theta + \varphi_1 - 2\kappa s_{1I})}, \quad (56b)$$

which shows that each pair of asymptotic solitons (u_i^+, u_i^-) have the same amplitudes.

- (ii) Since the center trajectories of all asymptotic solitons are along some curved lines in the xt' plane, u_i^\pm ($1 \leq i \leq 4$) have the t' -dependent velocities, namely,

$$v_1^\pm = -2|b|\rho + \frac{1}{2\rho\sqrt{1-b^2}|t'|}, \quad v_2^\pm = -2|b|\rho - \frac{1}{2\rho\sqrt{1-b^2}|t'|}, \quad (57a)$$

$$v_3^\pm = 2|b|\rho - \frac{1}{2\rho\sqrt{1-b^2}|t'|}, \quad v_4^\pm = 2|b|\rho + \frac{1}{2\rho\sqrt{1-b^2}|t'|}. \quad (57b)$$

The absolute differences $|v_1^\pm - v_2^\pm|$ and $|v_3^\pm - v_4^\pm|$ will increase when t' ranges from $+\infty$ to 0, which implies that the attraction between u_1^\pm and u_2^\pm (or between u_3^\pm and u_4^\pm) gradually gets strengthened in the near-field region. But as $|t'| \rightarrow +\infty$, $v_{1,2}^\pm \rightarrow -2|b|\rho$ and $v_{3,4}^\pm \rightarrow 2|b|\rho$, so that the asymptotic solitons u_1^\pm and u_2^\pm (u_3^\pm and u_4^\pm) tend to be parallel to each other in the far-field region.

(iii) There still exist the phase shifts for the envelopes of u_i^+ and u_i^- ($1 \leq i \leq 4$), and the phase differences can be given by

$$\delta\phi_1 = -\delta\phi_3 = -\ln \Xi_1^+ - \ln \Xi_1^- = -2 \ln[8\rho^2 b^2 (1-b^2)^{\frac{3}{2}} |t'|], \quad (58a)$$

$$\delta\phi_2 = -\delta\phi_4 = \ln \Xi_2^+ + \ln \Xi_2^- = 2 \ln[8\rho^2 (1-b^2)^{\frac{3}{2}} |t'|/b^2]. \quad (58b)$$

In contrast to the fixed phase shifts in Eq. (26), the absolute phase differences $|\delta\phi_i|$ in Eqs. (58a) and (58b) grow as $|t'|$ increases in the logarithmical manner (see Fig. 5).

From the above analysis, we can regard the soliton interactions in solution (28) are still *elastic* in the sense that the shapes and amplitudes of all interacting solitons are retained upon interaction, and that u_i^+ has the same velocity at t' as that of u_i^- at $-t'$. Although each asymptotic soliton profile could be either the dark or antidark type, solution (28) admits only four types of non-degenerate four-soliton interactions, as shown in Figs. 6(a)–6(d). Note that u_1^\pm and u_2^\pm always have the opposite soliton profiles, so do u_3^\pm and u_4^\pm (see Table 3). This is because the parametric conditions determining the soliton profiles of u_i^\pm ($1 \leq i \leq 4$) are not independent of each other. Besides, the four-soliton interaction can only degenerate to a two-soliton interaction, that is, both u_1^\pm and u_2^\pm vanish as $t' \rightarrow \pm\infty$ for $\sin(\varphi_1 - 2\kappa s_{1I}) = 0$, or both u_3^\pm and u_4^\pm vanish as $t' \rightarrow \pm\infty$ for $\sin(2\theta + \varphi_1 - 2\kappa s_{1I}) = 0$. In Figs. 7(a)–7(d), we depict all the four types of degenerate four-soliton interactions described by solution (28). Some small ripples can be observed in the near-field region, but they will eventually disappear as long as $|t'|$ is large enough. Accordingly, the degenerate cases cannot be regarded as the conventional two-soliton interactions, neither.

5 Conclusions and discussions

It has been shown in Refs. [14, 15] that the defocusing nonlocal NLS equation admits both the exponential and rational soliton solutions on the cw background $u_{cw} = \rho e^{i(2\rho^2 t + \phi)}$. In this paper, by using the twice-iterated DT and starting from the same seed u_{cw} , we have constructed two new types of exponential-and-rational mixed soliton solutions for Eq. (1) with $\varepsilon = -1$. Via the asymptotic analysis method, we have revealed that there are two exponential solitons and two rational ones in the first type of solution, and four mixed solitons in the second type of solution. The two types of solutions can exhibit a variety of elastic four-soliton interactions since each asymptotic soliton could be either the dark or antidark type. Also, we have discussed the degenerate cases when the four-soliton interaction reduces to a three-soliton or two-soliton interaction. For such two types of mixed soliton solutions, we have given the parametric conditions associated with all possible types of soliton interactions in Tables 1–3. Specially, we have revealed that

Table 3: Types of mixed asymptotic solitons in solution (28) with different parametric conditions.

Parametric conditions	u_1^\pm	u_2^\pm	u_3^\pm	u_4^\pm
$\text{sgn}(b) \sin(\varphi_1 - 2\kappa s_{1I}) > 0,$ $\text{sgn}(b) \sin(2\theta + \varphi_1 - 2\kappa s_{1I}) > 0$	MAD soliton	MD soliton	MAD soliton	MD soliton
$\text{sgn}(b) \sin(\varphi_1 - 2\kappa s_{1I}) > 0,$ $\text{sgn}(b) \sin(2\theta + \varphi_1 - 2\kappa s_{1I}) < 0$	MAD soliton	MD soliton	MD soliton	MAD soliton
$\text{sgn}(b) \sin(\varphi_1 - 2\kappa s_{1I}) < 0,$ $\text{sgn}(b) \sin(2\theta + \varphi_1 - 2\kappa s_{1I}) > 0$	MD soliton	MAD soliton	MAD soliton	MD soliton
$\text{sgn}(b) \sin(\varphi_1 - 2\kappa s_{1I}) < 0,$ $\text{sgn}(b) \sin(2\theta + \varphi_1 - 2\kappa s_{1I}) < 0$	MD soliton	MAD soliton	MD soliton	MAD soliton
$\text{sgn}(b) \sin(\varphi_1 - 2\kappa s_{1I}) > 0,$ $\sin(2\theta + \varphi_1 - 2\kappa s_{1I}) = 0$	MAD soliton	MD soliton	Vanish	Vanish
$\text{sgn}(b) \sin(\varphi_1 - 2\kappa s_{1I}) < 0,$ $\sin(2\theta + \varphi_1 - 2\kappa s_{1I}) = 0$	MD soliton	MAD soliton	Vanish	Vanish
$\sin(\varphi_1 - 2\kappa s_{1I}) = 0,$ $\text{sgn}(b) \sin(2\theta + \varphi_1 - 2\kappa s_{1I}) > 0$	Vanish	Vanish	MAD soliton	MD soliton
$\sin(\varphi_1 - 2\kappa s_{1I}) = 0,$ $\text{sgn}(b) \sin(2\theta + \varphi_1 - 2\kappa s_{1I}) < 0$	Vanish	Vanish	MD soliton	MAD soliton

the asymptotic solitons in the second type of solution have the t -dependent velocities and their phase shifts before and after interaction also grow with $|t|$ in the logarithmical manner, which is in sharp contrast with that in the local NLS equation. Finally, we would like to discuss the following issues:

- (i) It is a challenging work to find the sufficient and necessary nonsingular conditions for the soliton solutions of an integrable nonlocal equation [15, 43]. Although all the asymptotic solitons of solution (16) (or solution (28)) are globally nonsingular if and only if conditions (19) and (22) (or conditions (36) and (43)) are satisfied, it does not mean that solution (16) (or solution (28)) has no singularity with the same conditions. In fact, one may observe the singular phenomena in the near-field region $t \approx O(1)$ even if these conditions hold. Accordingly, Eqs. (19) and (22) (or Eqs. (36) and (43)) are just the *necessary* conditions for solution (16) (or solution (28)) to be nonsingular.
- (ii) For the exponential multi-soliton solutions, the asymptotic solitons are usually localized in some straight lines where there exists a balance between two or more dominant exponential terms of the tau function [44, 45]. But in deriving the mixed asymptotic solitons of solution (28), we develop

the asymptotic analysis method by considering the balance between some algebraic and exponential terms. It turns out that all the mixed asymptotic solitons of solution (28) are localized in some curves in the xt plane. In comparison, there is a well agreement between the asymptotic expressions and solution (28) when $|t| \gg 1$. Therefore, such method is valid and may be applicable to studying the asymptotic behavior of multi-soliton solutions for other nonlocal evolution equations [27–37].

Acknowledgement

This work was supported by the National Natural Science Foundation of China (Grant Nos. 11705284 and 61505054), by the Natural Science Foundation of Beijing Municipality (Grant No. 1162003), and by the Fundamental Research Funds of the Central Universities (Grant No. 2017MS051).

References

- [1] M. J. Ablowitz and Z. H. Musslimani, *Phys. Rev. Lett.* **110**, 064105 (2013).
- [2] V. V. Konotop, J. Yang and D. A. Zezyulin, *Rev. Mod. Phys.* **88**, 035002 (2016).
- [3] A. K. Sarma, M. A. Miri, Z. H. Musslimani and D. N. Christodoulides, *Phys. Rev. E* **89**, 052918 (2014).
- [4] T. A. Gadzhimuradov and A. M. Agalarov, *Phys. Rev. A* **93**, 062124 (2016).
- [5] M. J. Ablowitz and Z. H. Musslimani, *Nonlinearity* **29**, 915 (2016).
- [6] M. J. Ablowitz and Z. H. Musslimani, *Stud. Appl. Math.* **139**, 7 (2017).
- [7] M. J. Ablowitz, X. D. Luo and Z. H. Musslimani, *J. Math. Phys.* **59**, 011501 (2018).
- [8] M. J. Ablowitz, B. F. Feng, X. D. Luo and Z. H. Musslimani, *Theor. Math. Phys.* **196**, 1241 (2018).
- [9] M. J. Ablowitz, B. F. Feng, X. D. Luo and Z. H. Musslimani, *Stud. Appl. Math.* **141**, 267 (2018).
- [10] V. S. Gerdjikov and A. Saxena, *J. Math. Phys.* **58**, 013502 (2017).
- [11] Ya. Rybalko and D. Shepelsky, arXiv:1710.07961 (2017).
- [12] B. Yang and J. Yang, *Stud. Appl. Math.* **140**, 178 (2018).
- [13] A. Khare and A. Saxena, *J. Math. Phys.* **56**, 032104 (2015).

- [14] M. Li and T. Xu, *Phys. Rev. E* **91**, 033202 (2015).
- [15] M. Li, T. Xu and D. X. Meng, *J. Phys. Soc. Jpn.* **85**, 124001 (2016).
- [16] T. Xu, L. L. Li, M. Li and C. X. Li, “Asymptotic analysis of higher-order rational soliton solutions of the defocusing nonlocal nonlinear Schrödinger equation”, in preparation (2018).
- [17] X. Y. Wen, Z. Y. Yan and Y. Q. Yang, *Chaos* **26**, 063123 (2016).
- [18] Y. S. Zhang, D. Q. Qiu, Y. Cheng and J. S. He, *Rom. J. Phys.* **62**, 108 (2017).
- [19] X. Huang and L. M. Ling, *Eur. Phys. J. Plus* **131**, 148 (2016).
- [20] G. Q. Zhang, Z. Y. Yan and Y. Chen, *Appl. Math. Lett.* **69**, 113 (2017).
- [21] S. K. Gupta and A. K. Sarma, *Commun. Nonlinear Sci. Numer. Simulat.* **36**, 141 (2016); S. K. Gupta, *Opt. Commun.* **411**, 1 (2018).
- [22] B. Yang and J. Yang, arXiv:1711.05930 (2017).
- [23] B. Yang and J. Yang, arXiv:1712.01181 (2017).
- [24] M. Gürses and A. Pekcan, *J. Math. Phys.* **59**, 051501 (2018).
- [25] B. F. Feng, X. D. Luo, M. J. Ablowitz and Z. H. Musslimani, *Nonlinearity* **31**, 5385 (2018).
- [26] K. Chen and D. J. Zhang, *Appl. Math. Lett.* **75**, 82 (2018).
- [27] M. J. Ablowitz and Z. H. Musslimani, *Phys. Rev. E* **90**, 032912 (2014).
- [28] Z. Y. Yan, *Appl. Math. Lett.* **47**, 61 (2015); *Appl. Math. Lett.* **62**, 101 (2016); *Appl. Math. Lett.* **79**, 123 (2018).
- [29] D. Sinha and P. K. Ghosh, *Phys. Lett. A* **381**, 124 (2017).
- [30] Z. W. Wu and J. S. He, *Rom. Rep. Phys.* **68**, 79 (2016).
- [31] Z. X. Zhou, *Commun. Nonlinear Sci. Numer. Simulat.* **62**, 480 (2018).
- [32] J. L. Ji and Z. N. Zhu, *Commun. Nonlinear Sci. Number. Simulat.* **42**, 699 (2017).
- [33] A. S. Fokas, *Nonlinearity* **29**, 319 (2016).
- [34] V. S. Gerdjikov, G. G. Grahovski and R. I. Ivanov, *Theor. Math. Phys.* **188**, 1305 (2016).

- [35] C. Q. Song, D. M. Xiao and Z. N. Zhu, *J. Phys. Soc. Jpn.* **86**, 054001 (2017).
- [36] S. Y. Lou, *J. Math. Phys.* **59**, 083507 (2018).
- [37] S. Y. Lou and F. Huang, *Sci. Rep.* **7**, 869 (2017).
- [38] V. B. Matveev and M. A. Salle, *Darboux transformations and solitons* (Springer Press, Berlin, 1991).
- [39] C. H. Gu, H. S. Hu and Z. X. Zhou, *Darboux transformation in soliton theory and its geometric applications* (Shanghai Sci.-Tech., Shanghai, 2005).
- [40] V. B. Matveev, *Phys. Lett. A* **166**, 205 (1992).
- [41] B. L. Guo, L. M. Ling and Q. P. Liu, *Phys. Rev. E* **85**, 026607 (2012).
- [42] C. M. Bender and S. A. Orszag, *Advanced mathematical methods for scientists and engineers* (McGraw-Hill, New York, 1978).
- [43] T. Xu, M. Li, Y. H. Huang, Y. Chen and C. Yu, *Mod. Phys. Lett. B* **31**, 1750338 (2017).
- [44] G. Biondini and S. Chakravarty, *J. Math. Phys.* **47**, 033514 (2006).
- [45] T. Xu, C. J. Liu, F. H. Qi, C. X. Li and D. X. Meng, *J. Nonl. Math. Phys.* **24**, 116 (2017).
- [46] F. Genoud, *C. R. Math. Acad. Sci. Paris* **355**, 299 (2017).

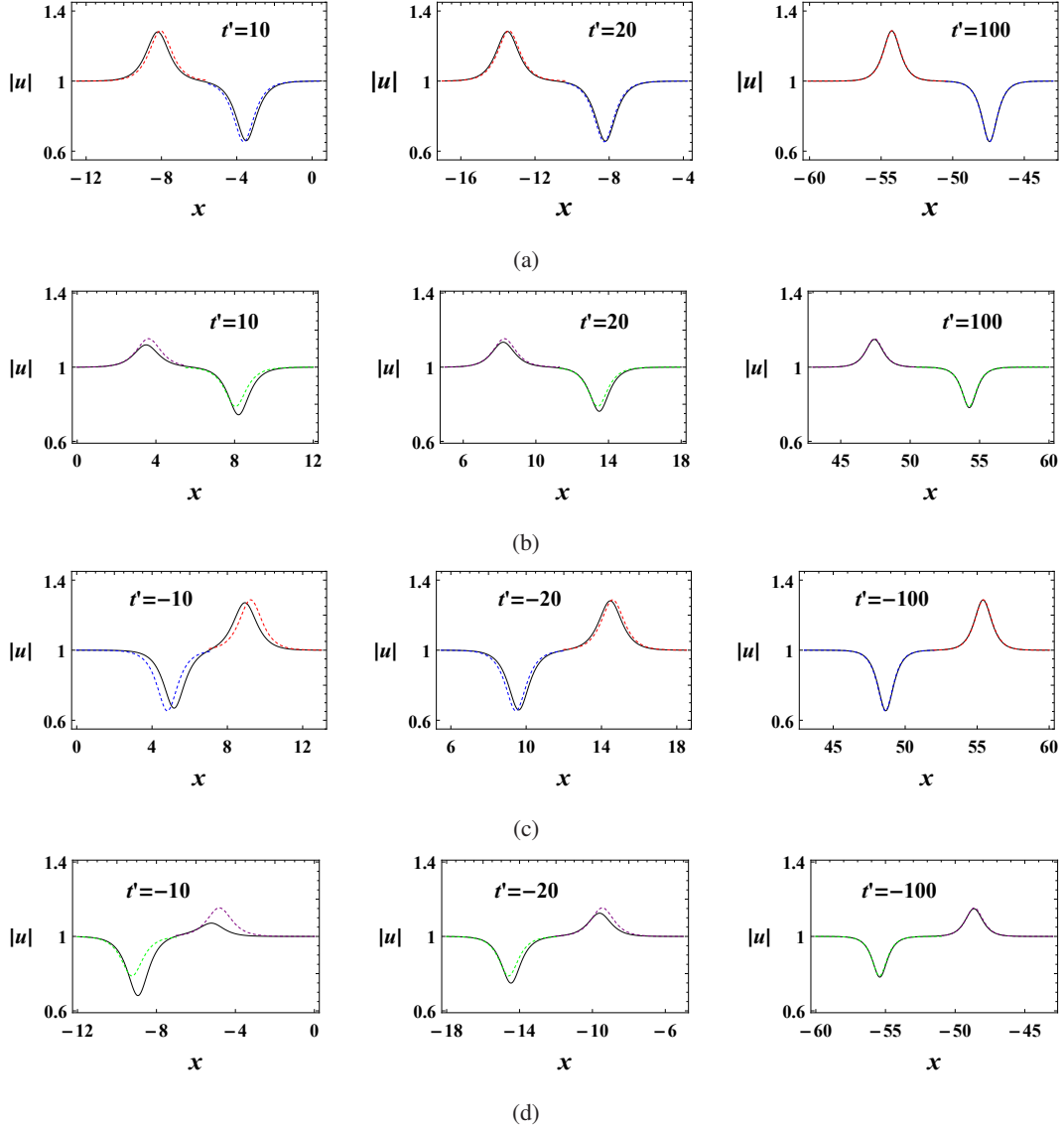


Figure 4: (a) Comparison of the asymptotic solitons u_1^+ (blue dashed) and u_2^+ (red dashed) with the exact solution (28) (black solid). (b) Comparison of the asymptotic solitons u_3^+ (purple dashed) and u_4^+ (green dashed) with the exact solution (28) (black solid). (c) Comparison of the asymptotic solitons u_1^- (blue dashed) and u_2^- (red dashed) with the exact solution (28) (black solid). (d) Comparison of the asymptotic solitons u_3^- (purple dashed) and u_4^- (green dashed) with the exact solution (28) (black solid). The relevant parameters are selected as $\rho = 1$, $b = \frac{1}{4}$, $\phi = 0$, $s_1 = 0$, $s_2 = 2$ and $\gamma_1 = 3 - i$.

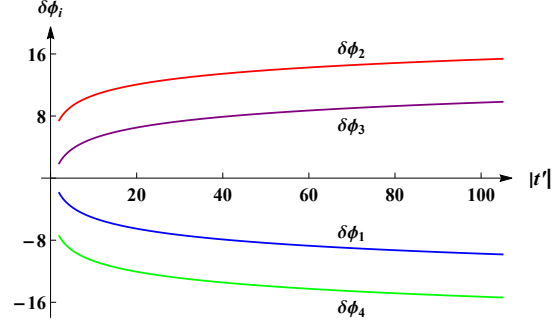


Figure 5: The phase differences for the envelopes of u_i^+ and u_i^- ($1 \leq i \leq 4$) versus t' , where the parameters are selected as $\rho = 1$, $b = \frac{1}{2}$ and $\phi = 0$.

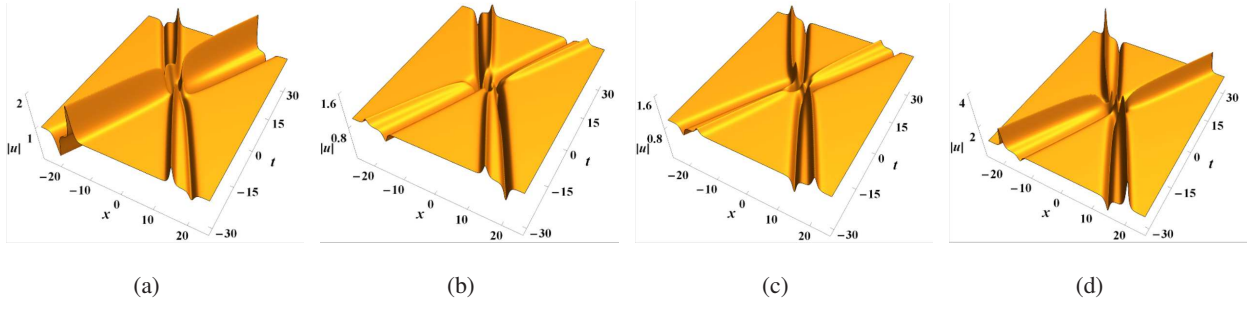


Figure 6: Four types of non-degenerate four-soliton interactions via solution (28): (a) MAD-MD-MAD-MD soliton interaction with $\rho = 1$, $b = \frac{1}{4}$, $\phi = 0$, $s_1 = 0$, $s_2 = 0$ and $\gamma_1 = 3 + i$. (b) MAD-MD-MD-MAD soliton interaction with $\rho = 1$, $b = \frac{1}{4}$, $\phi = 0$, $s_1 = 0$, $s_2 = \frac{1}{2}i$ and $\gamma_1 = -3 + i$. (c) MD-MAD-MAD-MD soliton interaction with $\rho = 1$, $b = \frac{1}{4}$, $\phi = 0$, $s_1 = 0$, $s_2 = 0$ and $\gamma_1 = 3 - i$. (d) MD-MAD-MD-MAD soliton interaction with $\rho = 1$, $b = \frac{1}{4}$, $\phi = 0$, $s_1 = 0$, $s_2 = 0$ and $\gamma_1 = \frac{1}{2} - i$.

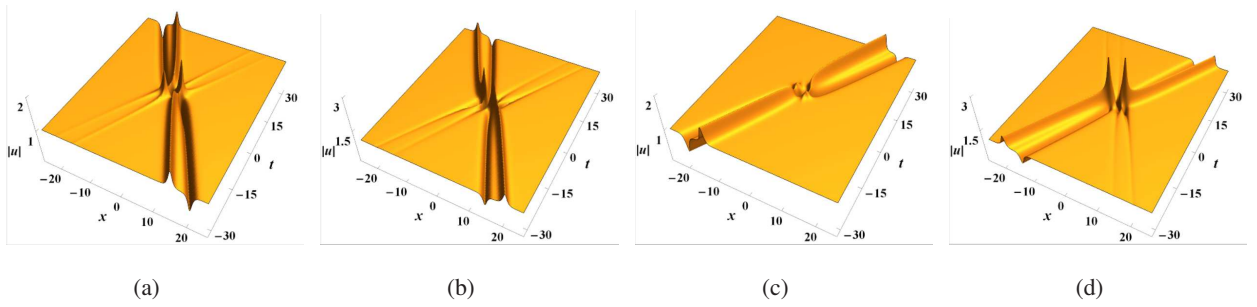


Figure 7: Four types of degenerate four-soliton interactions via solution (28): (a) MAD-MD-V-V interaction with $\rho = 1$, $b = \frac{1}{4}$, $\phi = 0$, $s_1 = 0$, $s_2 = \frac{1}{5}i$ and $\gamma_1 = -1 + \frac{\sqrt{15}}{7}i$. (b) MD-MAD-V-V interaction with $\rho = 1$, $b = \frac{1}{4}$, $\phi = 0$, $s_1 = 0$, $s_2 = \frac{3}{25}i$ and $\gamma_1 = 1 - \frac{\sqrt{15}}{7}i$. (c) V-V-MAD-MD interaction with $\rho = 1$, $b = \frac{1}{4}$, $\phi = 0$, $s_1 = 0$, $s_2 = 0$ and $\gamma_1 = 1$. (d) V-V-MD-MAD interaction with $\rho = 1$, $b = \frac{1}{4}$, $\phi = 0$, $s_1 = 0$, $s_2 = \frac{3}{25}i$ and $\gamma_1 = -1$. Here, “V” represents the vanishment of an asymptotic soliton as $|t| \rightarrow \infty$.